Norwegian University of Life Sciences
Faculty of Environmental Sciences and Natural Resource Management

2019
ISSN 2535-2806

MINA fagrapport 57

Estimating the size of the Scandinavian wolf population with spatial capture-recapture and conversion factors

Richard Bischof
Cyril Milleret
Pierre Dupont
Joseph Chipperfield
Mikael Åkesson
Henrik Brøseth
Jonas Kindberg

Bischof, R., Milleret, C., Dupont, P., Chipperfield, J., Åkesson, M., Brøseth, H., and Kindberg, J. 2019. **Estimating the size of the Scandinavian wolf population with spatial capture-recapture and conversion factors** - MINA fagrapport 57. 80 pp.

Ås, March 2019

ISSN: 2535-2806

AVAILABILITY
Open

PUBLICATION TYPE
Digital document (pdf)

QUALITY CONTROLLED BY
The Research committee (FU), MINA, NMBU

PRINCIPAL
Naturvårdsverket, Ref: NV-04566-17, Contact person: Jens Andersson

COVER PICTURE
Wolf (*Canis lupus*). Photo: Andrew Astbury/Shutterstock

NØKKELORD
Canis lupus, rovdyrforvaltning, omregningsfaktor, tetthet, deteksjonssannsynlighet, ikke-invaderende innsamling av genetisk materiale, åpen populasjon romlig fangst-gjenfangst, populasjonsdynamikk, ulv

KEY WORDS
Canis lupus, carnivore management, conversion factor, density, detection probability, non-invasive genetic sampling, open-population spatial capture-recapture, population dynamics, wolf

Richard Bischof (richard.bischof@nmbu.no), Faculty of Environmental Sciences and Natural Resource Management, Norwegian University of Life Sciences, PO Box 5003, NO-1432 Ås, Norway

Cyril Milleret, Faculty of Environmental Sciences and Natural Resource Management, Norwegian University of Life Sciences, PO Box 5003, NO-1432 Ås, Norway

Pierre Dupont, Faculty of Environmental Sciences and Natural Resource Management, Norwegian University of Life Sciences, PO Box 5003, NO-1432 Ås, Norway

Joseph Chipperfield, Faculty of Environmental Sciences and Natural Resource Management, Norwegian University of Life Sciences, PO Box 5003, NO-1432 Ås, Norway

Mikael Åkesson, Department of Ecology, Swedish University of Agricultural Sciences, Grimsö Wildlife Research Station, 73091 Riddarhyttan, Sweden.

Henrik Brøseth, Norwegian Institute for Nature Research, PO Box 5685, 7485 Trondheim, Norway.

Jonas Kindberg, Norwegian Institute for Nature Research, PO Box 5685, 7485 Trondheim, Norway.

Summary

Monitoring of wolves (*Canis lupus*) in Scandinavia is a coordinated effort between Swedish and Norwegian management authorities. Since 2012/13, the size of the Scandinavian wolf population is being estimated indirectly by applying a conversion factor to the number of detected reproductions (Box 1). This conversion factor (CF1) was calculated based on inventory data from 2001-2003. The intent to move from counting reproductions to counting the number of packs (family groups) in Sweden prompted the development of an updated conversion factor, which was published in 2016. This new conversion factor (CF2) was derived with an individual-based model of the wolf population that included social dynamics, information from telemetry studies, and a nearly complete pedigree.

Because CF2 differed from CF1 both methodologically and quantitatively, and due to the highly polarized debate surrounding wolf management in Scandinavia, management authorities sought to obtain another assessment via an independent analytical approach to evaluate the new findings. This motivated the analysis detailed in the present report. Specifically, the objective of this new analysis was to generate annual spatially explicit wolf population estimates and then use the results to derive the corresponding factor for converting the number of detected packs to the total number of individuals in the population.

We developed a Bayesian open-population spatial capture-recapture (OPSCR) model that incorporates 1) wolf population size and dynamics, 2) the spatial distribution and inter-annual movements of individuals, including dispersal, and 3) a detection process based on a combination of non-invasive genetic sampling (NGS) and recoveries of dead wolves. We then fitted this model to the extensive individual-based wolf monitoring data, which had been collected throughout the Scandinavian wolf range over five seasons (2013/14 to 2017/18) and compiled in the Scandinavian large carnivore database (Rovbase 3.0).

The OPSCR model yielded annual density maps, from which both total and jurisdiction specific population sizes were derived. Wolf population size estimates ranged between 368 (95% credible interval, CrI: 344 - 397) and 421 (CrI: 397 - 448) during the 5 year period of this study. The estimated number of wolves for October 1 2017 was 401 wolves (CrI: 392 - 412), of which 310 (CrI: 301-321) were located in Sweden and 91 (CrI: 83-101) in Norway. Based on numbers of observed packs reported for the five monitoring seasons, we arrived at a 5-year-median conversion factor (CF3, packs to total population size, October 1) of 8.8 (CrI: 8.2 – 10.0). Median annual conversion factors ranged from 8.6 to 9.8, with the conversion factor calculated for the 2017/2018 season (9.8; CrI: 9.6 - 10.1) being significantly higher than those during the previous four years. Although CF1 (9.2, uncertainty: 5.8 – 13.8; transformed for conversion from packs to population size), CF2 (8.2, CrI: 6.8 – 10.1, projected to October 1), and CF3 (8.8, CrI: 8.2 – 10.0) result in different point estimates of population size, comparisons between the three conversion factors is challenging, due to methodological differences, reliance on different data sources, and uncertainty reported (see Figure 15 on page 32).

The approach used here has several advantages over proxy-based approaches for obtaining estimates of population size. OPSCR models allow direct estimation of annual abundance from non-invasive genetic sampling and dead recovery data, while accounting for spatial and temporal variation in the detection probability of individuals. The resulting estimates are spatially explicit, allowing extraction

of abundance estimates and associated measures of uncertainty for any spatial extent desired by the user within the overall study area (*e.g.* at the country and county level), with October 1 as the reference date. Annual cause-specific mortality and recruitment are also estimated, both useful metrics of the population's status and trajectory. Importantly, this approach efficiently exploits the data (NGS and dead recoveries) currently collected annually by Swedish and Norwegian management authorities at the population and landscape level. Annual direct estimates of population size also circumvent potential problems arising from applying a fixed conversion factor when population structure or the proportion of detected packs changes over time.

For these reasons, and if economically and logistically feasible, we recommend the use of direct means for estimating population size when assessing the status of wolves in Scandinavia and evaluating the impact of management interventions. A transition from the use of proxies to direct population size estimation with the OPSCR model would entail a shift from pack and pair-centered monitoring to a less selective setup where effort is spread evenly enough to collect DNA samples throughout the population regardless of demographic (*e.g.* age) and social class (*e.g.* pup, scent-marking adult, vagrant). Whether such a shift is feasible, will depend on the amount of effort required to reach a desired level of precision and whether it allows monitoring of other population parameters that are of importance to managers. The observation process component of our OPSCR model most closely matched the NGS collection pattern during the 2017/18 monitoring season, which was the season with the most intensive data collection. Although such intensive monitoring may not be feasible on a long-term basis, results from a preliminary study, using the 2017/18 season as an example, suggests that reliable and precise population size estimates are still obtainable when monitoring intensity is reduced, as long as collection effort is spread across the landscape and all demographic/social classes. Further study is needed to assess the effort-precision tradeoff and to explore sampling design options that allow managers to obtain other measures of interest. We provide a discussion of the strengths and limitations of our approach, ideas for further development and study, and a series of recommendations for how to adjust the monitoring program to allow effective integration with the OPSCR approach for population size estimation.

Sammanfattning

Övervakning av varg i Skandinavien är en samordnad insats mellan svenska och norska förvaltningsmyndigheter. Sedan inventeringssäsongen 2012/13 har storleken på den skandinaviska vargpopulationen uppskattats indirekt med en omvandlingsfaktor (CF1) från antalet observerade föryngringar (motsvarande antal vargrevir med årsvalpar som överlever fram till 1 oktober). CF1 beräknades med data från inventeringsåren 2001-2003. I samband med en ändring från att räkna antalet föryngringar till antalet familjegrupper i Sverige utvecklades en uppdaterad omvandlingsfaktor som publicerades 2016. Denna nya omvandlingsfaktor (CF2) grundades på en detaljerad modell av vargpopulationen som inkluderade social dynamik och information från telemetri-studier samt ett nästintill fullständigt släktträd.

Eftersom CF2 skilde sig både i metodik och storleksmässigt från CF1, samtidigt som debatten om förvaltning av varg i Skandinavien är starkt polariserad, önskade förvaltningsmyndigheterna ytterligare en bedömning baserad på en oberoende analysmetod för att på detta sätt utvärdera de nya resultaten. Detta föranledde analysen som beskrivs i denna rapport. Syftet med denna nya analys är att ta fram årliga rumsligt kopplade uppskattningar av vargpopulationen och utifrån resultaten i modellen ta fram en faktor för att omvandla antalet observerade familjegrupper till det totala antalet individer i populationen.

Vi har utvecklat en Bayesiansk öppen spatial fångst-återfångstmodell (OPSCR) som inkorporerar 1) vargpopulationens storlek och dynamik, 2) individernas rumsliga fördelning och rörelse mellan år, däribland spridning, och 3) en detektionsprocess baserat på en kombination av icke-invasiv genetisk provinsamling (NGS) och återfunna döda vargar. Modellen anpassades till det omfattande individbaserade datamaterial som samlats in under övervakningen av hela det skandinaviska vargområdet under fem års tid (2013/14 till 2017/18) som ingår i en gemensam skandinavisk rovdjursdatabas (Rovbase 3.0).

OPSCR-modellen genererade årliga täthetskartor, från vilka vi tog fram både total och områdesspecifik populationsstorlek. Den årliga uppskattningen av populationsstorleken i Skandinavien varierade mellan 368 (95% trovärdighetsintervall, CrI: 344 - 397) och 421 (CrI: 397 – 448) vargar under den femårsperiod som studien baseras på. Den 1 oktober 2017 var populationsstorleken 401 vargar (CrI: 392 – 412), av vilka 310 (CrI: 301-321) befann sig i Sverige och 91 (CrI: 83-101) i Norge. Baserat på antalet observerade familjegrupper under de fem åren, kom vi fram till ett medianvärde för omvandlingsfaktorn (CF3, från familjegrupper till total populationsstorlek, 1 oktober) på 8,8 (CrI: 8,2-10,0). De årliga medianvärdena för omvandlingsfaktorn varierade mellan 8,6 och 9,8, där den senaste säsongen (2017/2018) hade ett värde (9,8; CrI: 9,6 – 10,1) som var signifikant högre än de tidigare fyra åren. Även om CF1 (9,2; CrI: 5,8 – 13,8; omräknad för omvandling från familjegrupper till populationsstorlek), CF2 (8,2; CrI: 6,8 – 10,1; uppskattad för 1 oktober), och CF3 (8,8; CrI: 8,2 – 10,0) återger olika punktuppskattningar av populationsstorlek, är det svårt att jämföra dem, p.g.a. skillnader i metodik, skillnader i dataunderlag och osäkerheterna som rapporterats (se figur 15, s. 32).

Det tillvägagångssätt som presenteras här har flera fördelar jämfört med tidigare metoder för att uppskatta populationsstorlek. OPSCR-modeller gör det möjligt att uppskatta täthet direkt från icke-invasiv genetisk provtagning samt återfångst av döda individer, samtidigt som hänsyn tas till rumslig

och tidsmässig variation i sannolikheten att detektera individer. Resultaten är uppskattningar som är rumsligt kopplade, vilket gör det möjligt att uppskatta täthet med en osäkerhet för vilket område som helst (t ex för ett land eller län) som ligger inom studieområdet, med 1 oktober som referensdatum. Modellen ger också årliga uppskattningar av dödlighet, specificerad till olika dödsorsaker, samt rekryteringsgrad, vilka båda är användbara indikatorer på populationens status och utveckling. Det är viktigt att poängtera att OPSCR-modellen på ett uttömmande sätt utnyttjar data (icke-invasiv provtagning och återfunna döda individer) som redan nu samlas in varje år på både populations- och landskapsnivå av svenska och norska förvaltningsmyndigheter. Med en årlig direkt uppskattning av populationsstorlek, som OPSCR-modellen ger, går det att undvika de problem som uppstår då en specifik omvandlingsfaktor används samtidigt som populationsstruktur och proportionen upptäckta familjegrupper förändras över tid.

Av denna anledning, föreslår vi, givet att det finns ekonomiska och andra resursmässiga förutsättningar, att populationsstorlek uppskattas direkt (istället för indirekt via en omvandlingsfaktor) för att utvärdera den skandinaviska vargpopulationens status och de förvaltningsåtgärder som bedrivs. För inventeringen, skulle en övergång från användandet av en omvandlingsfaktor till en direkt uppskattning av populationsstorlek med OPSCR-modellen innebära att övervakningen skulla behöva bli mindre fokuserad på att övervaka familjegrupper och par och istället fördelas så pass jämt över hela populationen så att DNA kommer att kunna samlas in från alla demografiska (t.ex åldersmässiga) och sociala grupper (t.ex. valpar, revirmarkerande vuxna och vandringsvargar). Huruvida detta går att åstadkomma beror på precisionen i populationsuppskattningarna som eftersträvas och i vilken mån det samtidigt går att se till att andra viktiga parametrar övervakas. Insamlingsmetoden som användes vintern 2017/2018 är den som bäst motsvarar de observationsprocesser som vår OPSCR-modell bygger på. Detta var inventeringssäsongen under studieperioden då datainsamlingen var som intensivast. Även om en sådan intensiv övervakning inte skulle vara möjlig framöver, visar dock preliminära studier från denna säsong, att pålitliga och exakta populationsuppskattningar går att ta fram även med en minskad insats, så länge insamlingen bedrivs över hela landskapet samt från alla demografiska och sociala grupper. Fortsatta studier behövs för att undersöka den avvägning som behöver göras mellan övervakningsinsats och precision i populationsuppskattningarna samt utvärdera olika utformningar på provinsamlingar som gör det möjligt för förvaltningen att även få information om andra viktiga populationsmått. Vi diskuterar styrkorna och begränsningarna med vår metodik, idéer för vidareutveckling och framtida studier samt en rad rekommendationer för hur övervakningen kan justeras för att bli bättre anpassad för populationsuppskattningar med OPSCR-modellen.

Table of Contents

1. Background 9
   1.1. Scandinavian wolf population 9
   1.2. Conversion factor and population size 9
   1.3. Objective and approach 10
2. Methods 13
   2.1. Data 13
      2.1.1. Non-invasive genetic samples (NGS) 13
      2.1.2. Dead recovery data 14
      2.1.3. Number of detected pairs and packs 15
      2.1.4. GPS search tracks 16
   2.2. Setup 17
      2.2.1. Temporal and spatial extent 17
      2.2.2. Scheduling 17
      2.2.3. Sex-specific analysis 18
   2.3. OPSCR model 18
      2.3.1. Population dynamics and population size 19
      2.3.2. Density, activity center locations, and movements 20
      2.3.3. Detections 21
   2.4. Analysis 24
   2.5. Parameter estimation 26
   2.6. Conversion factor calculation 26
   2.7. Model validation 27
3. Results 29
   3.1. Model performance 29
   3.2. Population size 29
   3.3. Conversion factor 31
   3.4. Detection probability 34
   3.5. Other parameters 34
4. Discussion 35
   4.1. Population size and conversion factors 35
   4.2. Search effort, detection probability, and precision 37
   4.3. Direct *vs.* indirect estimation of population size 38
   4.4. Recommendations for Scandinavian wolf monitoring 39
   4.5. Further development 40

5. Acknowledgements.....41
6. References 43

Appendices 1-7.......47

1. Background

1.1. Scandinavian wolf population

The Scandinavian wolf (*Canis lupus*) population has been increasing in size and range since a post-eradication founder event in 1983 (Wabakken et al. 2001b, Vilà et al. 2003). Today, wolves are again culled in both countries, with annual quotas or limits prescribed based on targets for abundance and present legislation. In recognition that wolves in Scandinavia are part of a transboundary population, Norway and Sweden have a history of collaboration and coordination in their wolf monitoring activities (Liberg et al. 2012), including a joint database (Rovbase.no).

Monitoring challenges, combined with intense scrutiny driven by the controversy surrounding wolf management, have led to today's approach to monitoring and expression of management goals. In both Sweden and Norway, the original aim was to monitor all individuals in the population, as well as the number and status of territories. The Swedish monitoring program changed as the wolf population grew. Vagrant wolves were no longer monitored when the population exceeded 100 individuals. Once the Swedish part of the wolf population exceeded 200 individuals, the number of wolves per pack was no longer monitored. Sweden has continued to monitor the number of packs, pairs and reproductions with the intent to follow population trends and estimate population size. Norway, with fewer wolves, has not changed its monitoring program during the same time period and still attempts to monitor all individuals in the population. For additional information about wolf monitoring and management in Scandinavia, see Liberg et al. (2012) and Chapron et al. (2016).

In both countries, monitoring consists of annual inventories using extensive search and tracking events. Evidence collected during the searches, including sources of DNA (primarily scat and urine, (Liberg et al. 2011), in combination with dead recoveries and detailed observations, have allowed the construction of a near complete pedigree (Liberg et al. 2005, Åkesson et al. 2016, Åkesson and Svensson 2018).

1.2. Conversion factor and population size

Stakeholders in Scandinavian wolf management require estimates of total population size. Population size is a key quantity in wildlife management, enabling the assessment of population status and evaluation of the outcome of management interventions. This motivated the establishment of a conversion factor from the number of detected reproductions to the total population size. The first conversion factor (CF1) was derived based on population inventory and resulting population estimates from monitoring seasons: 2000/2001, 2001/2002 and 2002/2003 (Wabakken et al. 2001a, 2002, 2004, Svensson et al. 2014). CF1 represents an average value over these 3 years: each reproduction counted during monitoring was assumed to represent 10 individuals in the population (see Appendix 1 for a description of the calculations leading to CF1 and the associated uncertainty boundaries). Since 2011, Swedish authorities have obtained wolf population size estimates indirectly through application of the conversion factor to the number of detected reproductions (Svensson et al. 2014).

A planned shift in Sweden towards monitoring packs only, instead of both reproductions and packs (for rationale see Chapron et al. 2016), has prompted the evaluation of the CF1. This led to the development of a second conversion factor (CF2, Chapron et al. 2016), which was derived using an individual-based model that incorporated a substantial amount of biological realism, including

population dynamics and sociality. This conversion factor (CF2: 8.0, 95% credible interval, CrI: 6.6 – 10.1) was lower than the one currently in use (at least in terms of their mean estimates), with potential consequences for wolf population size estimates and management in Sweden, including the setting of culling quotas. We note that CF2 is a factor for conversion from the number of packs to population size, whereas the original conversion factor is a multiplier of the number of reproductions. As CF2 entails a methodological and quantitative change (at least in terms of average difference from CF1), and due to the highly polarized debate surrounding wolf management, authorities sought to obtain another assessment via an independent analytical approach to confirm the new findings. Meanwhile, the original conversion factor (CF1) remains in effect for deriving annual wolf population size in Scandinavia from the number of observed reproductions. This assumes that the conversion factor calculated using data from 2001-2003 is still a valid expression of the ratio of detected reproductions to number of individuals in today's wolf population.

1.3. Objective and approach

The motivation behind the research detailed in this report is to allow managers to make a decision regarding the conversion factor and its use going forward. This requires information about wolf population size in order to calculate a factor for converting the number of detected packs into the total number of individuals in the population.

Given a monitoring program that is primarily concerned with detecting pairs and packs in Sweden, the principal challenge is estimating the number of pups and subadults within each pack and the number of individuals that are not part of a pack or pair (*e.g.* vagrants). We therefore focused our analysis on obtaining a direct and reliable estimate of population size and associated estimate of uncertainty, to form the basis for a new conversion factor from the number of detected packs to total population size. To do this, we developed a spatial capture-recapture (Efford 2011, Royle et al. 2013) model that integrates population dynamics and utilizes the information contained within the spatial configuration of detections and non-detections of wolves during genetic monitoring and dead recoveries. We chose this approach as it a) accounts for the individual and spatio-temporal variation in detection, b) captures the dynamics of the wolf population over time by estimating key vital rates, c) integrates multiple data sources in one comprehensive analysis, and d) makes spatially explicit predictions of abundance. The latter amounts to mapping population density across the landscape, which in turn permits extraction of the number of wolves for any spatial unit desired by the user, whether these are countries, counties, or other administrative entities. This aspect of the approach chosen here makes it particularly well suited for analyzing data from transboundary populations, which otherwise could lead to a mismatch between abundance estimates and the spatial extent they are attributed to (Bischof et al. 2016).

In the remainder of this report, we describe the analytical approach, present the results, and discuss our findings in the context of wolf monitoring and management in Scandinavia. We conclude with a series of recommendations for continued monitoring and the use of the resulting data in an adaptive management framework. The study described here was performed within the broader scope of project RovQuant, which is charged with the integrated analysis of monitoring data to guide adaptive management of large carnivores in Norway and Sweden (Bischof et al. 2017).

Box 1: Definitions and acronyms

Pack: Group of ≥3 wolves sharing a territory, including at least one scent-marking adult (Liberg et al. 2012). Also referred to as family group by the Scandinavian wolf monitoring program.

Territorial pair: Two scent-marking adults of opposite sex.

Vagrant: Non-territorial individual, having left its natal pack and not yet settled in a pair.

Pup: Individual aged 0–12 months, within its natal pack.

Subadult: Individual aged >12 months, remaining in its natal pack

Scent-marking adult: An individual that was identified at least once, during the current or any previous monitoring period, as a scent-marking member of a pack or a territorial pair.

Reproduction: We used the definition provided in Liberg et al. (2012): **"***For first time breeders, verification of a minimum of three wolves in the same territory is required, including a minimum of three tracking events during different days with a minimum of three wolves recorded at each event, and with each tracking event being minimum three km long. For packs that have bred before, the number of wolves should be minimum five wolves, or one wolf more than the year before (only applicable when there were 3 wolves in year t and 4 wolves in year t+1), to qualify as a reproduction, with the same minimum requirements for tracking as for first time breeders. Alternatively, a reproduction can be verified with aid of DNA, for example if all pups from the year before were DNA-typed, and the following year a new offspring from the same parents is identified in the territory, or if more pups are identified by DNA in one year than the maximum number of individuals tracked in the same territory the year before. For first time breeders, it is enough if only one offspring is identified with aid of DNA*."

Recruits: Number of pups that survive until the start of the monitoring period (October 1) in their birth year.

CF: Conversion factor; multiplier for calculating total wolf population size from the number of detected packs or reproductions.

Legal culling: Lethal removal of wolves by legal means, including licensed recreational hunting, management removals, defense of life and property.

Pedigree: The ancestry of each individual linking back to the original founders of the population. The pedigree consists of individual identities linked to the identity of both parents (if known).

AC: Activity center. Equivalent to the center of an individual's home range during the monitoring period. "AC location" refers to the spatial coordinates of an individual AC in a given year, and "AC movement" to the movement of an individual AC between consecutive years.

CR: Capture-recapture.

SCR: Spatial capture-recapture.

OPSCR: Open-population spatial capture-recapture.

CrI: 95% credible interval associated with a posterior sample distribution. See also Box 2.

CI: 95% Confidence interval.

MCMC: Markov Chain Monte Carlo.

NGS: Non-invasive genetic sampling.

2. Methods

2.1. Data

This study integrates information from multiple sources, the primary one being the Scandinavian large carnivore database Rovbase 3.0 (rovbase.no; last extraction 2019-02-12). This database is used jointly by Norway and Sweden to record detailed information associated with large carnivore monitoring, including, but not limited to, non-invasive genetic sampling (NGS) data, dead recoveries, GPS search tracks, and carnivore observations. The following is a description of the various types of data used in the analysis.

2.1.1. Non-invasive genetic samples (NGS)

Swedish and Norwegian management authorities - Statens naturoppsyn (SNO, Norway) and Länsstyrelserna (Sweden) - conduct annual searches (Section 2.1.4) for sources of DNA (primarily scats and urine) throughout the Scandinavian wolf range. Although samples may be collected any time of the year, the official survey period starting with the 2014/15 season has been October 1 – March 31. The 2013/14 sample collection season ended one month earlier (October 1 – February 28). About one third (30%) of DNA samples originate from opportunistic searches (without associated information on search effort) conducted by hunters or other members of the public.

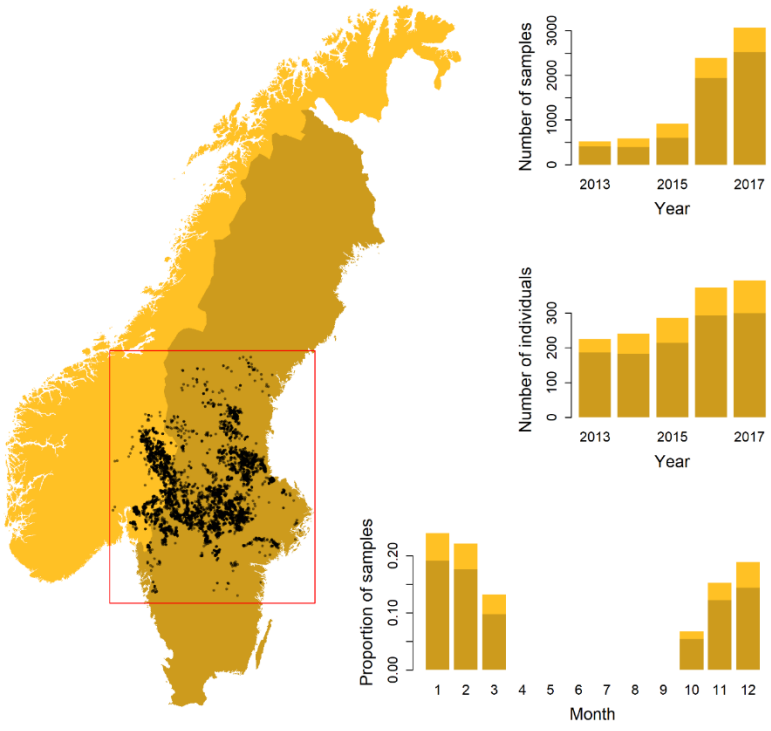

Figure 1. Spatial and temporal distribution of NGS samples from wolves used in the OPSCR analysis. The red polygon defines the spatial extent of the study area considered in the analysis. Only samples included in the analysis are shown.

Samples collected are analyzed by isolating DNA followed by genotyping 1) 90 autosomal single nucSNPs, 5 SNPs linked to the X chromosome and one diagnostic marker on the male-specific Y chromosome using '96.96 Dynamic array Chip for Genotyping' (Fluidigm Inc., San Francisco, USA) and modified protocol provided by Fluidigm (Åkesson et al. 2018) and 2) up to 30 microsatellite markers using PCR followed by fragment length separation using capillary electrophoresis (see Åkesson et al. 2016 for details). The sample genotypes were used to determine species, population origin (*i.e.* Scandinavian or Finnish/Russian wolf), individual identity, parental identities and sex (Åkesson et al. 2018). A common database of genotypes is shared and continuously updated between the DNA laboratory at Grimsö Research Station (SLU, Sweden) and the Norwegian Institute for Nature Research (NINA, Norway).

All NGS samples for which coordinates, detection dates, species, individual ID (genotype), and sex are available were used in the analysis. We further restricted the analysis to samples collected during the primary survey period (Oct 1 and March 31) between 2013/14 – 2017/18 within the pre-defined study area that contained the entire Scandinavian wolf breeding range. These restrictions resulted in a dataset composed of 7478 detections from 851 identified individuals (Figure 1; Appendix 2, Tables A2.1 and A2.2).

2.1.2. Dead recovery data

DNA from dead carnivores, if genotyped, can be linked with NGS data via individual IDs and provide definite information about the fate of individuals. We used data on dead recoveries between October 2013 and March 2018 in the analysis (Figure 2).

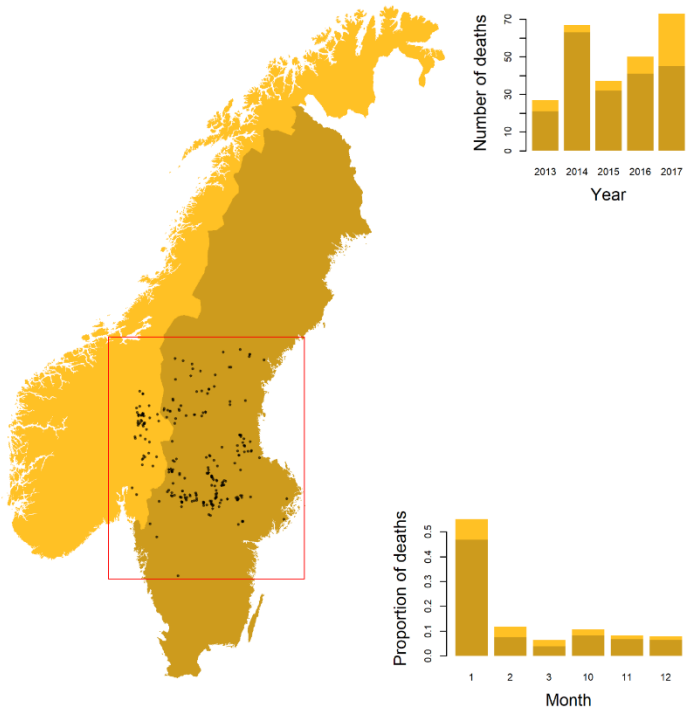

Figure 2. Spatial and temporal distribution of dead recoveries of wolves between Oct 2013 and March 2018 within the spatial extent considered in this analysis (red polygon). Only dead recoveries included in the analysis are shown.

All deaths due to legal culling (*e.g.* legal hunting, management kills, defense of life and property) have to be reported to the authorities. Although some mortalities due to other reasons (*e.g.* natural deaths, vehicle and train collisions, illegal hunting) are also reported, an unknown proportion remains undetected. All wolves legally culled (N=280) were DNA identified, as well as most individuals recovered dead from other causes of mortality (N=55, Appendix 2, Table A2.3). Furthermore, dead carnivores in Scandinavia are often aged via cementum annuli counts, which allows for reconstruction of individual life histories (*i.e.* minimum year of recruitment into the population). Dead recoveries are a valuable source of information that can be integrated in OPSCR models, improving model performance and the reliability of parameter estimates (RovQuant, unpublished results). Finally, dead recoveries associated with GPS-coordinates provide additional information for the estimation of individual locations, especially valuable for individuals with few or no alive detections.

2.1.3. Number of detected pairs and packs

Each year, field observations, genetic sampling data, dead recoveries, and the resulting near-complete pedigree of the Scandinavian wolf population are used to establish counts of pairs, packs, and reproductions (Svensson et al. 2014, 2015, 2017, 2018, Wabakken et al. 2016; Figure 3; Appendix 2, Table A2.4). The social status (adult scent-marking member in a pack, adult scent-marking member in a pair or subadult member of a pack) was determined on a yearly basis for identified individuals using the pedigree and track information from the monitoring. The identity of known adult scent-marking individuals are reported in the yearly monitoring reports (Svensson et al. 2014, 2015, 2017, 2018, Wabakken et al. 2016). Offspring to first-time reproducing pairs that were identified within the first year of their life (1 May to 30 April of the following year) were reported as juvenile members of the family group. The number of detected packs was used to calculate conversion factors from population size estimates yielded by the OPSCR model.

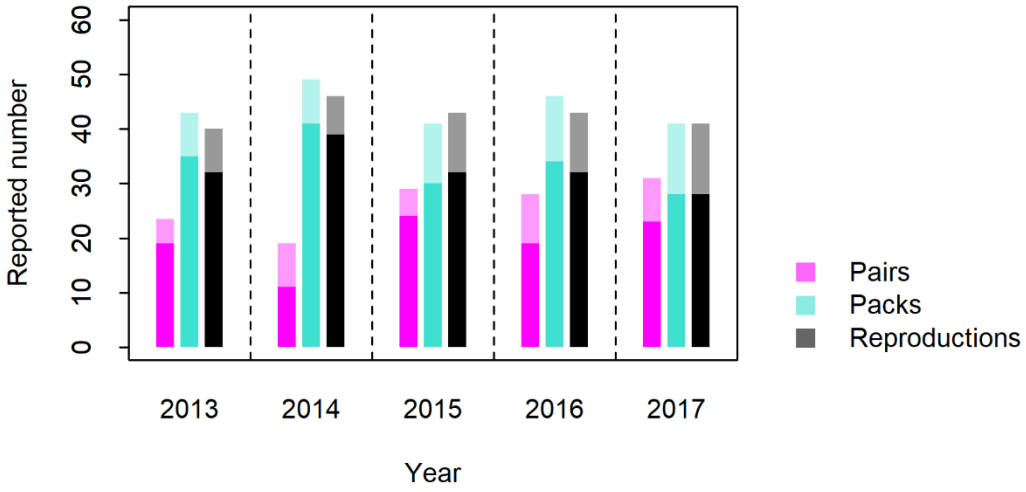

Figure 3. Number of detected wolf pairs, packs, and reproductions, as reported by the monitoring program for seasons 2013/14 to 2017/18. Darker shaded bars indicate numbers associated with the Swedish part of the wolf population.

2.1.4. GPS search tracks

In Sweden, each County Management Board (Länsstyrelse) is responsible for finding packs and pairs within its jurisdiction (county). This is done either by searching for tracks on snow, or scats on bare ground along forest roads or smaller roads or by receiving reports from hunters, reindeer herders and the public. When searching along roads, the search route is logged and later imported into Rovbase. Found tracks are followed with the intent to discover information on the number of wolves and territorial markings. All tracking events are logged and later imported into Rovbase. In Norway, the system is the same but searches are performed by SNO and Inland Norway University of Applied Sciences. As the majority of DNA samples are collected during these searches, the GPS logs are highly detailed records of the spatial configuration and intensity of the annual monitoring effort. GPS search tracks are included in the OPSCR model to account for spatial and temporal variation in search effort (Section 2.3.3). Opportunistic samples collected by hunters and other members of the public are not associated with direct information about search effort, but other proxies for detectability can be used in the form of spatial covariates, such as distance from roads or snow cover (see Section 2.3.3). Overall, 611 000 km of GPS tracks were recorded in the study area during the five monitoring seasons included in this study (Figure 4).

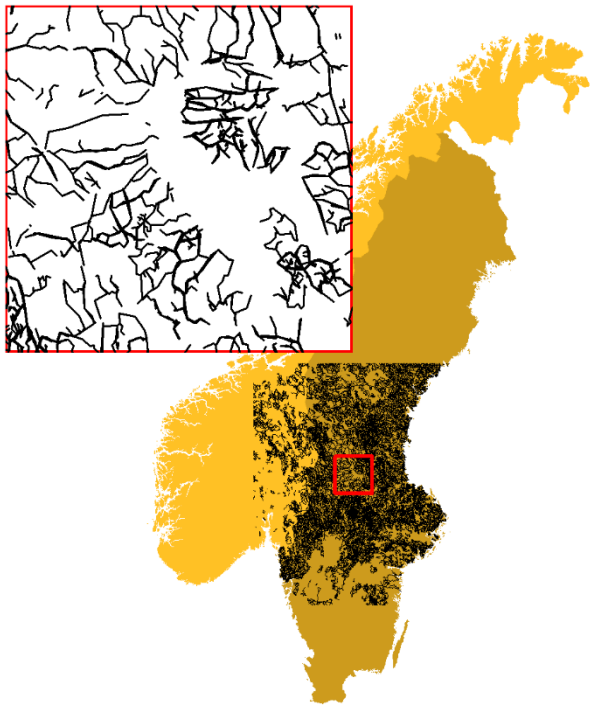

Figure 4. Map of tracks logged by searchers during the 2017/18 wolf monitoring season in Norway and Sweden (total length = 226 000 km). The cutout shows tracks within the 100x100km red square located in central Sweden.

During the monitoring seasons 2016/17 and especially during 2017/18, Swedish management authorities implemented intensified DNA collection protocols involving both Länsstyrelserna and the Swedish Hunters Association. Länsstyrelserna collected every DNA sample they found during searches along roads and during snow tracking. Hunters voluntarily collected samples found in the hunting area.

In addition, during 2017/18, Länsstyrelserna followed a different search program. The goal was to search every 5x5 km grid cell at least twice for a total of at least 25 km per cell, while aiming to collect DNA samples from all demographic and social classes.

2.2.Setup

2.2.1. Temporal and spatial extent

The empirical analysis of wolf data focused on five monitoring seasons between 2013/14 and 2017/18. Official starting and end dates for monitoring were October 1 and March 31, respectively. Although wolves occur throughout Scandinavia, we had to delineate a reasonably constrained study area (E9.18, N57.65 - E19.82, N63.50; Figure 5) in order to make the computation associated with the OPSCR model tractable. This region encompasses the wolf breeding range and most of the wolf detections/dead recoveries (99%). After removing contiguous non-land and urban areas (>80 km^2), we ended up with a habitat polygon of 259 700 km^2. We subdivided that region into a grid of 10x10 km cells to define the available habitat used in our analysis.

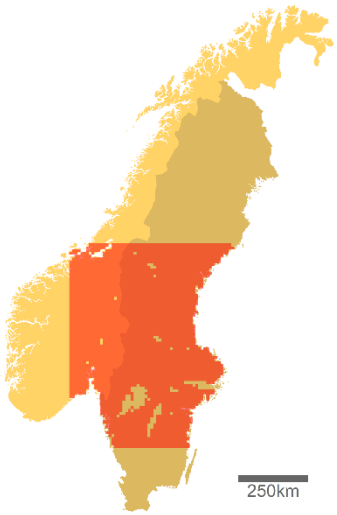

Figure 5. Spatial extent (E9.18, N57.65 - E19.82, N63.50) of suitable habitat considered in the analysis, colored in red.

2.2.2. Scheduling

The timing of events in the lives of individuals that make up the population needs to be reflected in the scheduling of population dynamic models and has important implications for the interpretation of estimates. A simplified annual life cycle for wolves in Scandinavia is shown in Figure 6. Our OPSCR model uses the annual monitoring season as a core element in its scheduling. The start of the monitoring season (October 1) is the point in time to which the estimates of population status (*i.e.* abundance estimates) are linked. From the model's perspective, transitions between individual states (*e.g.* survival and recruitment, see Section 2.3.1), and thus changes in abundance, occur after March 31 and before October 1. Although in reality, changes also occur throughout the monitoring season, the resulting violation of population closure assumption has been shown to have negligible consequences for medium to long-lived species (Dupont et al. 2019).

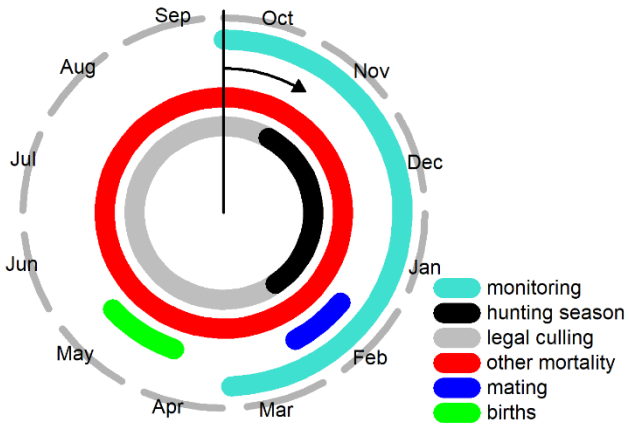

Figure 6. Timing of life history events and monitoring in the Scandinavian wolf population. The start of the monitoring period and direction of time flow are indicated by a vertical black line and an arrow at October 1, respectively. Although the main legal culling period is associated with the hunting season (black), legal culling can occur throughout the year (grey/black). Estimated dates of mating and births are based on Alfredèen (2006) *and Nonaka* (2011).

2.2.3. Sex-specific analysis

We implemented separate OPSCR models for males and females, instead of a combined-sex model, for several reasons: a) OPSCR models pose a substantial computational challenge, particularly when applied at the level of landscapes and population as in our analysis (Milleret et al. 2018b, 2018a), and the computational burden rapidly increases with increasing number of individuals in the study population. By splitting the population in a male and female populations, independent models can be run simultaneously, significantly reducing the total time needed for model fitting; b) because of sex-specific traits in wolves, most parameters in the model (*e.g.* detection probability, survival, dispersal) would need to be estimated separately.

2.3. OPSCR model

We built an open-population spatial capture-recapture (OPSCR; Ergon and Gardner 2014, Bischof et al. 2016) model composed of three sub-models:

1) A model for population dynamics and population size.
2) A model for AC locations and AC movements.
3) A model for individual detections during DNA searches.

To be effective, ecological modelling requires a balance between realism and simplicity. Ultimately, a model should be no more complex than it has to be to achieve its primary objective. Increased realism comes at the cost of higher complexity, loss of generality, and the risk of not being able to detect the most important process(es). In our case, increased realism and complexity also incur a substantial increase in computational burden, potentially prolonging the process of model fitting by weeks or months. During the work described here, we strove to include essential processes that either proved to have pronounced consequences for model predictions or that we considered indispensable based

on prior information about the system and preliminary analyses. In the following sections, we describe each model component. For additional details and mathematical notation, see Appendix 3.

2.3.1. Population dynamics and population size

We modeled annual population dynamics as transitions between individual states (Figure 7, Bischof et al. 2009). Between two consecutive years, an individual remains either in its current state or transitions to another one, with transition probabilities determined by vital rates (*e.g.* recruitment and mortality). Here we considered five different states (see Appendix 3 for additional details). An individual can be:

1) "unborn" if it has not yet entered the population (for modeling recruitment)

2) "alive other" if it is alive and has not yet been observed as a scent-marking member of a pair or pack (Box 1).

3) "alive scent-marking adult" if it is alive and has either presently or previously been observed as a scent-marking member of a pair or pack.

4) "dead legal" if it has died from legal culling (which includes legal hunting, Figure 6) between the start of the previous and current monitoring seasons.

5) "dead": if it has a) died from any other cause of mortality between the start of the previous and current monitoring seasons or b) died earlier, regardless of the cause.

In the model, an individual is recruited by transitioning from state "unborn" to state "alive other". In subsequent years, it can either become a pair member (transition to state "alive scent-marking adult") or remain in its current state. A scent-marking individual may leave its pack or pair, but, due to our definition of states 2 and 3, once an individual has entered state 3 ("alive scent-marking adult") it cannot return to state 2 ("alive other"). Finally, both individuals in states 2 and 3 may die, either from legal culling (transition to state 4 "dead legal"), or from all other causes of mortality (transition directly to state 5 "dead"). Once in state 4, the individual must transition to state 5 in the next time step, which is the final, absorbent state (Figure 7). Total population size in each year is the sum of all individuals in alive states (states 2 and 3).

We distinguished between two alive states (2-3) to account for differences in detectability and demography. Once wolves have reached maturity, they generally establish a territory with another mature individual of the opposite sex (state 3) and leave scent-marks (*e.g.* urine, scats) that facilitate the collection of DNA material. Although death of one sex can occur, individual turn-over is common and ensures the maintenance of the territorial pair (Milleret et al. 2016). Additionally, high site fidelity facilitates detection of territorial individuals during subsequent monitoring seasons (see for example wolf territory maps in Svensson et al. 2017, 2018). This distinction between states in the model serves capture potential differences in survival and detection parameters between different segments of the population.

We consider two competing sources of mortality: legal culling, which is always detected (*e.g.* legal hunting, management kills, defense of life and property and all other mortalities, which may not always be detected (*e.g.* natural deaths, vehicle and train collisions, verified illegal hunting). By

distinguishing between these two kinds of mortalities in the model and accounting for imperfect detection, the OPSCR model can produce estimates of total mortality, as well as separate estimates for each mortality type (Bischof et al. 2009).

All vital rates were allowed to vary between years, yielding annual estimates of recruitment (number of pups born and surviving to October 1), transition from "alive other" to "alive scent-marking adult", and state and cause-specific mortality. All vital rates were estimated separately for males and females in sex-specific OPSCR models (see Section 2.2.3).

Further description of the state transition process and associated transition probabilities is provided in Appendix 3.

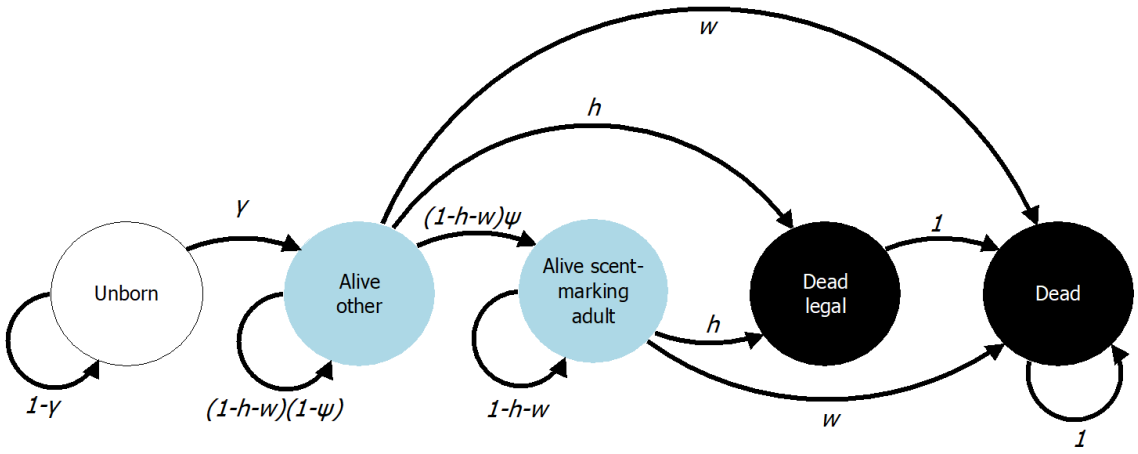

Figure 7. Diagram illustrating the transitions between states in the multi-state model of population dynamics. Circles depict the five possible states an individual can be in. Arrows represent transitions from one state to another and variables shown next to arrows represent the probabilities of these transitions; the probability of being recruited into the population from the unborn state (γ), the probability to die from legal culling (h), the probability to die from all other causes (w) and the probability to become a confirmed adult scent-marking member of a pair or pack (ψ). For the purposes of the analysis, once an individual has been designated by the monitoring program as a scent-marking member of a pair or pack, it remains in that state until it dies, even if, biologically, scent-marking individuals may become solitary again.

2.3.2. Density, activity center locations, and movements

In OPSCR, the location of an individual is described by the location of its activity center (AC, Box 1), which is equivalent to the center of a circular home range. The AC location of a detected individual in a given year is informed by the spatial configuration of detections of this individual across the landscape. The AC location of individuals that were not detected are determined based on the spatial heterogeneity in detection probability and a spatial covariate describing the distribution of activity centers within the study area (Appendix 3). Undetected individuals are less likely to be placed where detection probability is high. The region shown in Figure 5 is the area within which the OPSCR model can allow ACs to be located.

Individual AC locations may shift over time, due to factors such as dispersal but also adjustments in landscape use or changes in territorial boundaries. The OPSCR model allows AC movements between

years, ranging from no movement to long distance dispersal. Similar to the initial AC location model, the distribution of AC movement distances is informed by the spatial distribution of detections of individuals detected in multiple years. The model generates an estimate of the median inter-annual AC movement distance (Appendix 3).

Wolves can select specific habitat types when establishing a territory (Ordiz et al. 2015, Sanz-Pérez et al. 2018), but because the pack is the functional unit within which reproduction is occurring, the density of individuals is strongly linked to the spatial distribution of packs. We therefore used the annual density of known packs as a proxy for the AC placement intensity surface across the landscape (Appendix 2, Figure A2.6).

2.3.3. Detections

Although individual detections can occur continuously in the landscape, it is common to aggregate individual detections to the closest point (detector) in a grid. The OPSCR model accounts for imperfect detection, *i.e.* the fact that an individual could not be detected at every detector throughout the study area and the possibility that some individuals remained completely undetected. In SCR modelling (Figure 8), detection is closely linked with the home range concepts in that the probability of detecting an individual declines with increasing distance from its AC location. This is an oversimplification of reality, where detection probability may not be normally distributed within an individual's home range and may drop off abruptly beyond the boundaries of a territory.

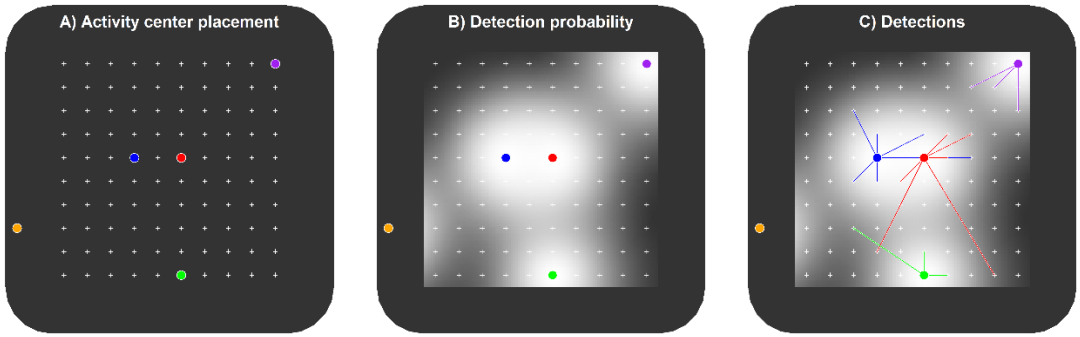

Figure 8. Schematic representation of the spatial capture-recapture process: A) Distribution of individual AC locations (colored dots) across the study region (black area: available habitat; white dots: detectors). B) Heat map of a detection function describing the relationship between detection probability and distance to AC (lighter shading = higher detection probability, Figure 9). C) Realization of detections (color-coded segments linking individual detections to their respective ACs).

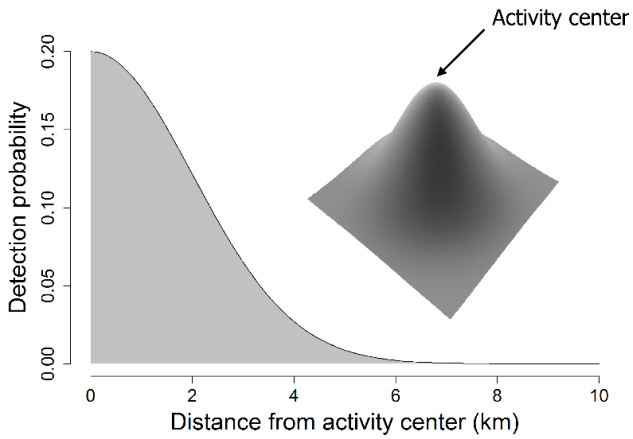

Figure 9. Illustration of the half-normal detection function (left) describing decreasing detection probability with distance from the AC location. The detection function is directly related to the utilization distribution around an individual's activity center (right). The baseline detection probability (p_0) is the intercept and is equal to 0.2 in this example. The scale parameter (σ) of the function dictates its shape and the speed at which the function decreases. For details, see Appendix 3.

The detection function (*e.g.* the half-normal detection function, Figure 9) is a core element in spatial capture-recapture models and enables the estimation of latent (unobserved) AC locations, based on the spatial configuration of detectors and individual detections. Detectors in our study are represented by the center of cells in a spatial grid (10x10km main detector cells; each divided into 100 1x1 km sub-detector cells, Figure 10, Milleret et al. 2018b). The likely position of an individual's AC is determined based on the spatial pattern of its detections and non-detections across the detector grid. On the other hand, some individuals with ACs in the study area may not be detected at any detector. This is dealt with in the model by data augmentation (Royle et al. 2007, 2009). The use of the state "unborn" allows for inclusion of individuals in the population that have remained undetected during monitoring ("available" individuals that transition to "alive"). Through data augmentation, the model is provided with additional individuals that were not detected, but that may be part of the population (see Appendix 3).

We considered a habitat buffer of 40km around the detector grid (Figure 10). The buffer area allows placement of individual AC locations, but does not contain any information about individual detections. This is an important component of SCR models, as it allows the movement of individuals in and out of the study area (Efford 2011, Royle et al. 2013, Gardner et al. 2018).

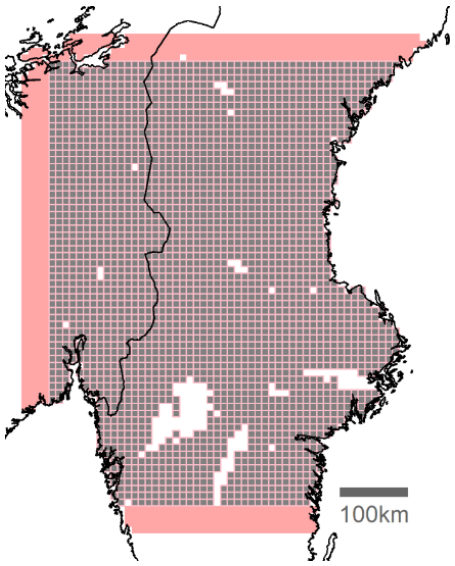

Figure 10. Map of the detector grid used in the analysis. Each detector grid cell (10x10km, grey squares) is further subdivided into 100 1x1km sub-detector cells (not shown here). Individual detections are spatially aggregated to the centroid of the closest detector cell. The habitat (shaded red area) extends 40km beyond the edge of the detector grid.

Detection probability is informed from the detections and non-detections of individuals that were detected at least once. From this, the probability that an individual that is present in the population remains undetected at any detector is derived. The model can thus not only predict the likely location of detected individuals, but also the presence and distribution of undetected individuals. Both the baseline probability (p_0) and shape parameter (σ) of the detection function can be under the influence of individual and spatial, detector-specific factors. We included the following effects on the baseline detection probability:

Detector-level covariates:

- Length of search tracks logged by searchers within each detector grid cell in each monitoring period (Appendix 2, Figure A2.6): this variable was included as a linear covariate on the baseline detection probability.
- Average distance from the nearest road (Appendix 2, Figure A2.6): the distance from each detector to the closest road (1:100 000, Lantmäleriet, Sweden; N50 kartdata, Statens kartverk, Norway). This variable represents accessibility, which we predict to facilitate detectability.
- Average monthly percentage of snow cover in each detector grid cell (MODIS, https://neo.sci.gsfc.nasa.gov, accessed 2018-12-14; monthly, at 0.1 degrees resolution; (Appendix 2, Figure A2.6)) during each monitoring period (October 1- March 31). As wolf NGS relies heavily on the presence of snow, we predicted that greater snow cover increases detectability.
- Jurisdiction: to control for differences in monitoring regimes between jurisdictions (counties) we estimated independent baseline detection probabilities for each county. Counties on the edge of the study area with only a few detections were merged with neighboring counties to yield sufficiently large sample sizes for reliable estimation of the baseline detection probability (see Appendix 7, Figure A7.6).

Individual covariates:

- Wolves are territorial animals occupying similar areas over consecutive years. Therefore, prior detection is expected to positively influence the probability of being detected at subsequent occasions. This is referred to as “trap-response” or “trap-happiness” in the capture-recapture literature (Williams et al. 2002). To account for this, we used an indicator of whether an individual was detected or not during previous monitoring season as a linear predictor of the baseline detection probability.
- Monitoring, especially in Sweden, is focused on scent-marking group members, as their presence defines the presence of pairs or packs. Being territorial, these individuals are also actively scent-marking within their home ranges, thus facilitating the collection of urine or scats. Therefore, being designated as a scent-marking pair or pack member should increase the overall probability of detection of those individuals. For this reason, we modelled separate baseline detection probabilities for individuals in states “alive scent-marking adult” and “alive other” (Section 2.3.1).

In addition to these covariates, we estimated different baseline detection probabilities for each annual monitoring period to control for temporal variation in search effort. Detection probability and the effect of the aforementioned individual and spatial factors were estimated separately for males and females in the sex-specific OPSCR models (Section 2.2.3).

2.4.Analysis

We fitted our Bayesian OPSCR models using Markov chain Monte Carlo (MCMC) simulation with NIMBLE (Turek et al. 2016, de Valpine et al. 2017, NIMBLE Development Team 2019) in R version 3.3.3 (R Core Team 2018). NIMBLE provides a new implementation of the BUGS model language coupled with the capability to add new functions, distributions, and MCMC samplers to improve computing performance. We ran four chains, each with 10000 iterations, including a 3000-iteration burn-in period. A brief description of the MCMC process and its outcome is provided in Box 2. We used a computing cluster (https://cigene.no/tag/orion) for running each MCMC chain on a separate core, ultimately enabling us to run many chains simultaneously thereby reducing the total time required to obtain results. We considered models as converged when the Gelman-Rubin diagnostics (Rhat, Gelman 1996) was ≤1.1 for all parameters and by visually inspecting the trace plots.

OPSCR models represent a significant computational challenge due to the potentially millions of calculations involved. This challenge is amplified in our analysis because the model is unusually complex (multiple processes, many parameters estimated) and due to the size of the problem (number of individuals and spatial extent). For this reason, during project RovQuant we have developed approaches and implemented a number of features to substantially reduce computation time, thereby enabling us to run complex OPSCR models in a few days, instead of months. These developments include:

1. Spatial aggregation: We developed a new observation model that allowed us to substantially reduce the number of detectors (and therefore runtime) without compromising precision and accuracy of model estimates (Milleret et al. 2018b; Appendix 3).

2. Local evaluation: We reduced the number of calculations to be performed by removing unnecessary evaluation of the likelihood whenever the distance between a detector and a predicted AC location was larger than a distance threshold (Milleret et al. 2018a).
3. NIMBLE: We moved model implementation from JAGS (Plummer 2003) to NIMBLE (NIMBLE Development Team 2019). NIMBLE compiles the model into machine code and thus allows for faster computation compared to software that requires the model definition to be parsed to an interpreter at run time. The flexibility of NIMBLE also allowed us to implement the aforementioned developments as timesaving NIMBLE functions.

Box 2: Bayesian models & Markov chain Monte Carlo

The OPSCR model was implemented in a Bayesian framework with Markov chain Monte Carlo (MCMC) simulations. Non-informative or mildly informative prior distributions were provided for all parameters that are to be estimated by the model. The MCMC procedure draws parameter values from their prior distribution and evaluates the resulting model fit to the data. Over many thousand iterations of this process, the model-drawn parameters move towards values that lead to improvements in the model fit to the data. For each model, multiple chains are run, *i.e.* the MCMC sampling process is repeated with different starting values, resulting in different trajectories of parameters. Eventually, as model-sampled parameters approach values that are most likely given the data, the different MCMC chains will have converged. Instead of a single value for each parameter, this type of model returns a distribution of MCMC samples for each parameter of interest. Using these so-called posterior samples, we calculate the median value for each parameter distribution, as well as the associated 95% credible interval (*i.e.* the range of posterior values between 2.5% and 97.5% of the posterior distribution). Any measure derived from a model-estimated parameter (such as the conversion factor) inherits the characteristics of the posterior distribution(s) of the constituent parameter(s), thus also yielding a measure of uncertainty for the derived parameter.

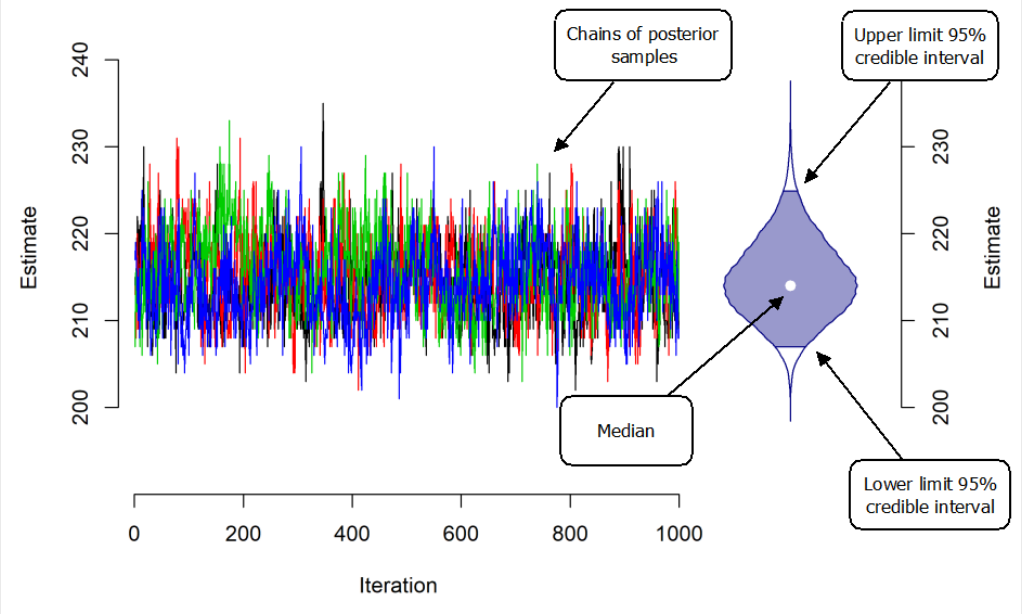

2.5. Parameter estimation

The OPSCR is a complex hierarchical model, with many parameters estimated. Population size and the conversion factor derived from it were the focus of the analysis, but we monitored additional parameters because they can be of interest from a management perspective or because they helped track model behavior and validate assumptions. These parameters included cause-specific mortality (legal culling and other causes), recruitment, inter-annual movement distance, and home range size.

The number of OPSCR-predicted AC locations (live individuals) per habitat cell within a given region sums to the total predicted number of wolves within that region. In this fashion, abundance estimates and the associated uncertainty can be extracted for any desired spatial unit, including country or county level estimates. For a full list of parameters estimated with the OPSCR model, see Figure 11 and Appendix 4 (Table A4.1). For all parameters, we report the median and the 95% credible interval limits of the posterior distribution. Combined (female/male) parameter estimates were obtained by merging the posterior samples of the sex-specific models.

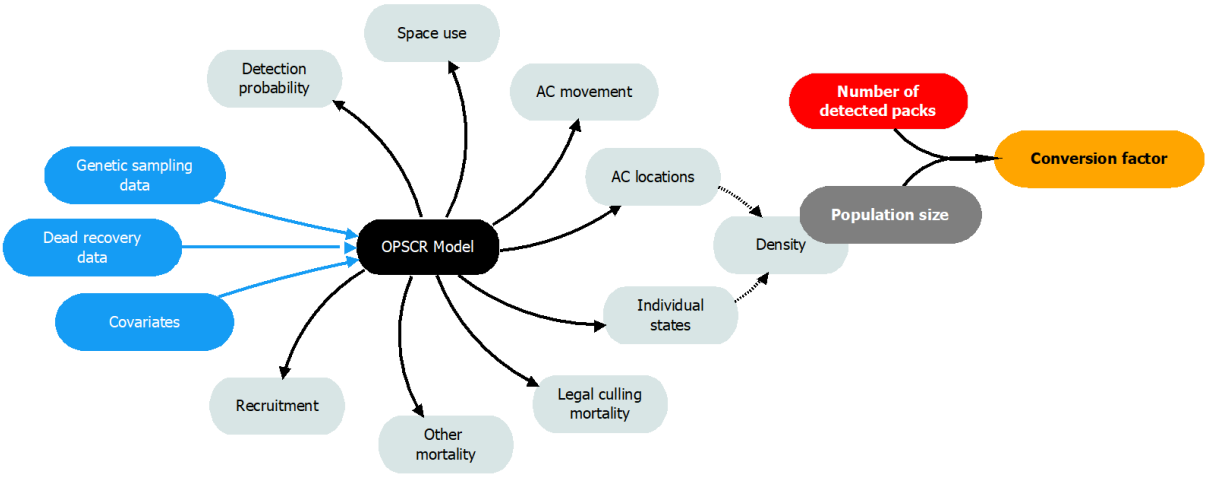

Figure 11. Diagram of OPSCR model inputs (blue bubbles) and outputs (grey bubbles). Density and population size are derived variables, calculated from model-estimated parameters. The factor for converting the number of detected packs to population size is derived from the OPSCR-estimated population size and the number of detected packs documented by the monitoring program.

2.6. Conversion factor calculation

The conversion factor from observed number of packs to total population size was calculated by dividing annual population size estimates by the number of detected packs in the same year (as reported in Svensson et al. 2014, 2015, 2017, 2018, Wabakken et al. 2016; Figure 3).

Comparisons between the three available conversion factors (CF1, CF2, and CF3) are not straight forward, due to the different approaches used to obtain them. CF1 was derived based on a reported number of reproductions detected between October 1 and March 31, and therefore can be considered to refer to October 1 (animals that die during the monitoring period are counted as part of the abundance estimate in the focal year, as they were part of the population on October 1). Although

CF2 was originally reported for December 1, the model by Chapron et al. (2016) allows estimation of the conversion factor for any month of the year and can be used to derive a conversion factor for October 1. As requested by the Swedish management authorities, CF3 is a multiplier of the number of detected packs, whereas CF1 is a multiplier applied to the number of detected reproductions. CF2 was derived using the number of packs estimated by the model of Chapron et al. (2016) and not the number of detected packs. Although Chapron et al. (2016) found that there is an approximately one-to-one relationship between the number of packs and number of reproductions, the number of detected packs and reproductions reported by the monitoring program do not always align (Figure 3), which would amplify differences in population size derived with a conversion factor.

To facilitate comparison between alternative conversion factors, we a) obtained an alternative version of CF1 based on the reported number of detected packs (and not reproductions, calculated using the information presented in Appendix 1) and b) re-projected CF2 based on the monthly model-predicted wolf population composition on October 1 instead of December 1 (Chapron et al. 2016). This resulted in the following versions of CF1 and CF2 for conversion from the number of detected packs to total population size:

- CF1: 9.2 (5.8 – 13.8); point estimate and uncertainty bounds are calculated as for the original CF1, but based on the number of detected packs (see also Appendix 1).
- CF2: 8.2 (CrI: 6.8 – 10.1); based on predictions from the model by Chapron et al. (2016) for October 1.

2.7. Model validation

The OPSCR model and its components are the result of multiple cycles of developments and tests. Before accepting each new model or model extension, we performed extensive simulations for a wide range of parameter values. We then fit the model to these simulated datasets and compared model-generated estimates with simulated parameter values. The goal of these tests was to determine if the model performs well (*i.e.*, low bias, high precision) under the conditions it was designed for. As part of a series of simulation studies, we also evaluated the model's sensitivity to likely violations of the assumptions of population closure and independence between individuals. To assess how well the model fit the empirical wolf data, we conducted qualitative evaluation of model predictions using comparisons with previously known attributes, and a goodness of fit analysis using Bayesian posterior predictive checks (Gelman and Shalizi 2013). For a detailed description of the model validation process, see Appendices 5 and 6.

3. Results

3.1. Model performance

Fitting the OPSCR model to simulated data produced population size estimates with high accuracy (relative bias 2%) and precision (coefficient of variation < 0.03, Appendix 5; Figures A5.3 and A5.4). Earlier studies by project RovQuant also provided indication that spatial capture-recapture models are robust to violations of assumption of population closure (Dupont et al. 2019) and independence in the spatial configuration of individuals (RovQuant unpublished results). Bayesian posterior predictive checks revealed reasonably close resemblance between model-predicted data and the empirical data used in the analysis (Appendix 6, Figures A6.1 and A6.2). However, we suggest further analysis to precisely quantify the goodness of fit of our model, and to assess the potential consequences of poor fit for the accuracy and precision of our estimates.

3.2. Population size

The model-estimated median population size for the entire study area (259 700 km^2, excluding the buffer area) ranged between 368 (2013 and 2015) and 421 (2014) individuals, depending on year (Figure 12). The estimated population size for October 1, 2017 was 401 (CrI: 392 – 412). Based on the predicted location of ACs, we estimated that in 2017, 310 wolves (CrI: 301-321) could be attributed to Sweden and 91 (CrI: 83-101) to the Norway. Whereas the estimated number of wolves in Sweden fluctuated without a clear upward or downward trend, we detected a steady increase in the Norwegian part of the wolf population during the study period (Figure 12, Appendix 7, Table A7.1). The association of population size with sub-regions of the study area is illustrated in Figure 13. A further breakdown into annual county and sex specific estimates is provided in Appendix 7 (Table A7.2). Note how the greater number of detections associated with the increased survey effort after the 2015/16 season led to higher precision in estimates of population size (Figure 12) and other parameters (Appendix 7).

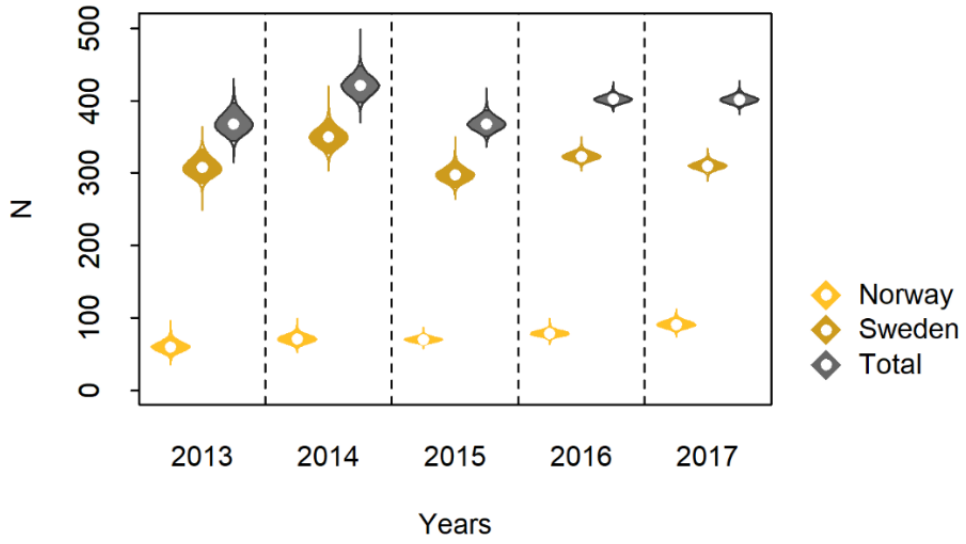

Figure 12. Total and country-specific annual wolf population size estimates from the OPSCR model within the study area. Violins show the posterior distribution of the annual population size estimates (points: medians; solid colors: 95% credible interval).

The open population SCR model yielded annual density maps (Figure 14), which illustrate changes in the distribution of individuals over time. Average density in 2017 was estimated as 0.154 wolves per 100 km^2 (CrI: 0.151 – 0.159) throughout the 259 700 km^2 study area.

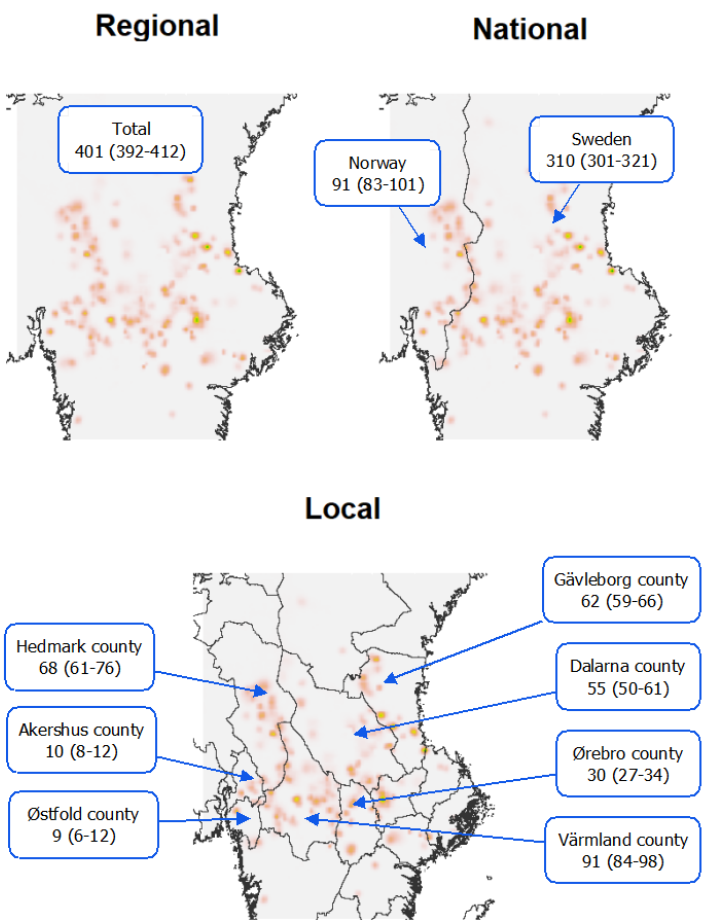

Figure 13. Maps showing the OPSCR-estimated wolf population density for Oct. 1, 2017 in Scandinavia with regional, national, and local (county) delineations. Total and jurisdiction-specific estimates of wolf population size can be derived for any spatial extent within the study area; examples are provided in the boxes (with 95% credible intervals in parentheses). Not all counties are shown, therefore county estimates do not add up to national totals.

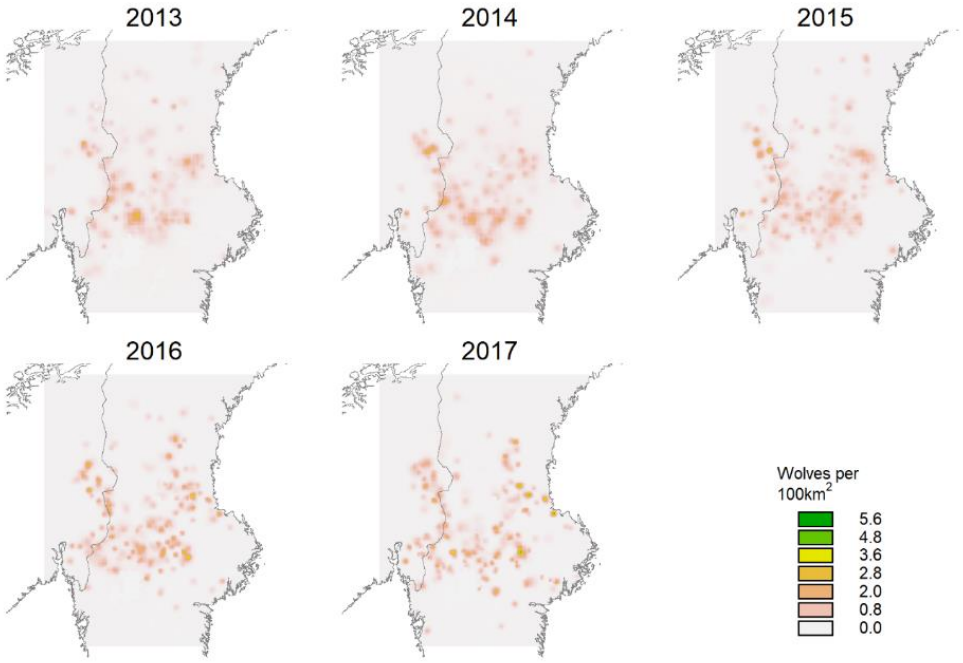

Figure 14. Maps of annual wolf density derived from the OPSCR model.

3.3. Conversion factor

Based on annual Scandinavian wolf population size estimates and the number of packs reported by the monitoring program each year, we estimated the annual conversion factor from detected packs to total number of individuals to range from 8.6 (CrI: 8 - 9.2) to 9.8 (CrI: 9.6 - 10.1) over the five-year study period (Table 1, Figure 15). This results in a 5-year median conversion factor of 8.8 (CrI: 8.2 - 10.0; calculated from the combined posteriors of the five years). Like total population size estimated here and the number of detected packs reported by the monitoring programs, the conversion factor refers to the configuration of the population on October 1 each year. The estimated conversion factor was significantly greater in 2017 than during the preceding years (Table 1).

Table 1. Number of packs reported annually by the monitoring program between 2013 and 2017, median OPSCR-estimated population size for the same year, and the resulting annual number of individuals in the population per detected pack (conversion factor). Credible intervals (95%) are shown in parentheses.

Year	Number of detected packs	OPSCR-estimated population size	Conversion factor (CF3)
2013	43	368 (344 - 397)	8.6 (8.0 - 9.2)
2014	49	421 (397 - 448)	8.6 (8.1 - 9.1)
2015	41	368 (351 - 387)	9.0 (8.6 - 9.4)
2016	46	402 (393 - 412)	8.7 (8.5 – 9.0)
2017	41	401 (392 - 412)	9.8 (9.6 - 10.1)
5-year median			**8.8 (8.2 – 10.0)**

Note that that the uncertainty around our estimate of the annual conversion factor originates solely from the distribution of the posterior estimate of population size. Any potential uncertainty in the number of detected packs is not reported, and hence does not contribute information about uncertainty around the conversion factor. Therefore, the uncertainty reported around the conversion factor should be interpreted as a lower uncertainty value, because the combined uncertainty associated with the number of packs and the population size estimate is either equal or greater. Although wolf population size estimates derived using CF2 are lower than estimates derived with CF1 and CF3, wide uncertainty bands around the estimates do not allow discerning of significant differences (Figure 16).

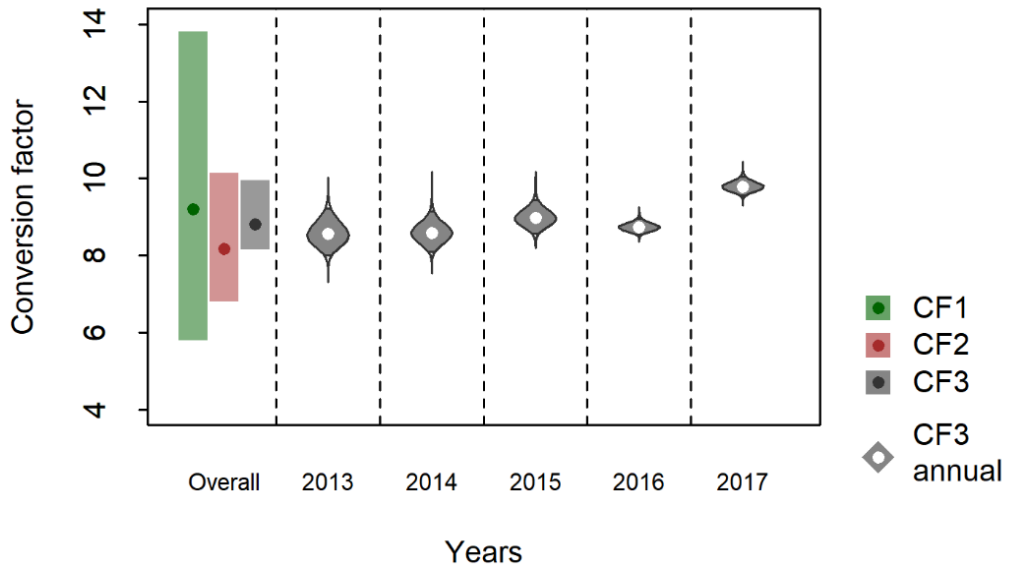

Figure 15. Annual variation in the conversion factor (CF3, grey violins, detected packs to total population size) derived using annual wolf population size estimates from the OPSCR model and the reported number of detected packs each year. Colored points with bars on the left show multi-year averages/medians of a) the conversion factor currently in use (CF1, green), the conversion factor by Chapron et al. (2016; CF2, red)*, and the 5-year median of our estimate (CF3, grey/black). For comparison purposes, CF1 was recalculated based on the number of detected packs, instead of the number of reproductions.*

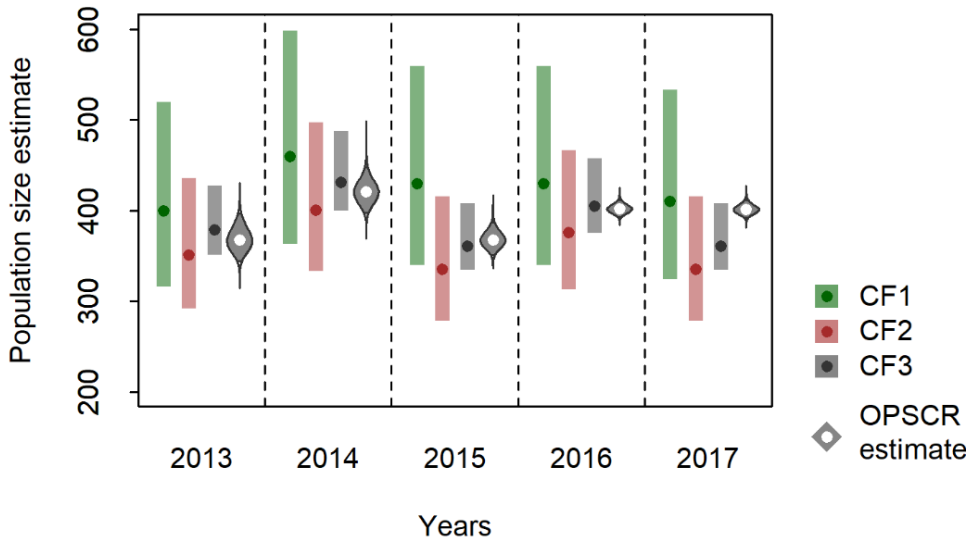

Figure 16. Annual wolf population size estimates predicted by the OPSCR model (grey violins) and population size estimates derived using conversion factors CF1 (applied to number of detected reproductions; green point: mean, green bar: uncertainty range), CF2 (applied to the number of detected packs; red point: median, red bar: CrI), and CF3 (applied to the number of detected packs; black point: median, grey bar: CrI). Median CF3 and CrI where calculated from the joint posterior of all five years of the study.

The population size estimate obtained with the OPSCR model can also be used to calculate 5-year median conversion factors from other indices, such as the number of detected pairs, the combined number of detected packs and pairs, and the number of reproductions. Comparison of the resulting predictions with the annual OPSCR-estimated population size estimate suggests that conversion factor-based population size estimates from the number of detected packs and reproductions most closely track the OPSCR population size estimates, while a conversion from pairs is less reliable and associated with the highest uncertainty (Figure 17).

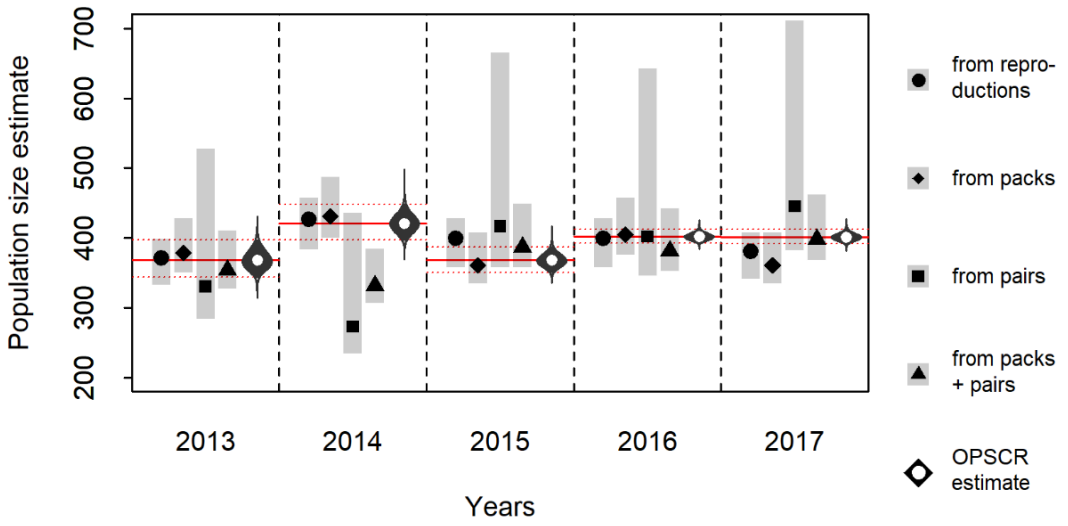

Figure 17. Population size estimates using variants of the 5-year median CF3 for conversion to total wolf population size from the number of detected reproductions, the number of detected packs, the number of detected pairs, and the combined number of detected packs and pairs. The OPSCR population size estimate is shown for comparison, with solid and dashed red lines indicating the median and CrI, respectively. Symbols indicate medians, vertical bars 95% credible intervals.

3.4. Detection probability

The baseline detection probability (*i.e.* the probability of detecting an individual exactly at its AC location) varied between counties, generally increased with time, was higher for males than females and for individuals that had been identified as scent-marking members of pair or pack vs. those that had not (Appendix 7). Detection probability increased with the length of recorded search trails (males: β = 0.27, CrI: 0.24 - 0.31; females: β = 0.27, CrI: 0.23 - 0.3) and decreased in areas further away from roads for both males (beta = -0.52, CrI: -0.74 - -0.33) and females (β = -0.85, CrI: -1.11 - -0.59). The average proportion of snow cover had no significant effect on the baseline detection probability for either sex (males: β = -0.01, CrI: -0.1 - 0.08; females: β = 0.07, CrI: -0.04 - 0.18). Detection probability increased significantly in Sweden during the two seasons with intensified NGS (Appendix 7). Detection probability was also generally higher for individuals if they had already been detected during a previous period (males: β = 0.12, CrI: 0.02 - 0.23; females: β = 0.37, CrI: 0.26 - 0.48).

3.5. Other parameters

Results for additional parameters estimated with the OPSCR model are provided in Appendix 7 (Tables A7.3 and A7.4).

4. Discussion

4.1. Population size and conversion factors

Using a hierarchical analysis that integrated both non-invasive sampling data and dead recoveries, we estimated that the annual size of the Scandinavian wolf population ranged between 368 (CrI: 344 - 397) and 421 (CrI: 397 - 448) during the 5-year study period (Figure 12). The estimated number of wolves for the 2017/2018 season was 401 wolves (CrI: 392 - 412), of which 77% (CrI: 75% – 79%) were located in Sweden. Based on population size estimates from the OPSCR model and the number of packs detected during five monitoring seasons (2013/14 – 2017/18), we derived a 5-year-median conversion factor (CF3) of 8.8 (CrI: 8.2 – 10.0) for calculating total population size from the number of detected packs. In addition to a direct estimate of annual population size and density, the OPSCR model also yielded estimates of annual cause-specific mortality, recruitment, space use, movement, as well as measures of the effect of individual and environmental covariates on certain parameters (Appendix 7). These parameters were not the focus of the present analysis and are not discussed here, but are nonetheless important population metrics.

The transformed versions of CF1 (based on the number of packs instead of reproductions) and CF2 (referring to October1 instead of December 31), allow for limited quantitative comparison of all three conversion factors (Figure 15), with two important caveats: i) the three conversion factors were based on data from different years (CF1 from 2001-2003, CF2 from 2003/04 to 2014/15, and CF3 from 2013/14 to 2017/18) with differences in sampling design and intensity, and ii) uncertainty estimates are difficult to compare due to substantial differences in the underlying models/calculations. While CF2 and our model derived credible intervals, it is unclear what kind of uncertainty the range presented with CF1 quantifies (Appendix 1). Although the approach leading to CF2 also provides the uncertainty in the number of packs (not done for CF1 and CF3), this information is not currently available to managers when implementing a conversion factor based on documented packs. Aside from differences in methods and data used, the reported uncertainty intervals of the three conversion factors overlap extensively, limiting inferences about their differences in magnitude.

We focus the comparison of approaches for estimating population size on the approach by Chapron et al. (2016; CF2) and the approach described in this report (CF3). We think that without a re-calculation of the original conversion factor (CF1) using updated survey data that represent the recent characteristics of the population, and a more robust approach for estimating uncertainty, further evaluation of that method will be of limited use.

The model by Chapron et al. (2016) presents a flexible and effective approach to population size estimation for a species with a complex and dynamic social structure. Chapron et al. (2016) modelled population and social dynamics with a high level of realism. This included transitions between different age and social classes, and associated vital rates. Furthermore, their model yielded estimates of state variables and the conversion factor through the year (monthly). In our approach, we traded off some of these features for the added ability to make spatially explicit predictions at the population level and a joint estimation of all parameters from individual detection data.

Imperfect detection. Neither the analysis that led to the original conversion factor (CF1), nor the model by Chapron et al. (2016, CF2) accounted for imperfections in the observation process, *i.e.* the fact that individuals (in any social category and demographic group) could remain undetected or their demographic status misidentified. CF1 was calculated using minimum and maximum counts of

individuals obtained during monitoring seasons 2000/01-2002/03 (Appendix 1). Although it may be possible to expand the approach leading to CF2 by making it hierarchical (G. Chapron, pers. comm. 2019-03-14) and thus account for imperfections in the count data inputs, the current version requires reliable information about initial population size and composition, together with vital rate estimates to simulate multiple stochastic population trajectories/dynamics. After simulating a very large number of population trajectories, only simulations that yielded numbers of pairs, packs and reproductions close to the reported numbers were retained to derive CF2. The assumption of this approach for estimating absolute population size is that all packs, pairs and reproductions are detected. If the approach is only to be used to estimate the conversion factor, but not abundance, the assumption is that detectability is constant across social categories and through time. By contrast, our OPSCR model assumes an underlying latent ecological process (true abundance and distribution of individuals in the population), which is linked with detection data through an observation model. Temporal and spatial heterogeneity in detectability is thus estimated and accounted for.

Population and landscape scale. To parameterize their model (via highly-informative priors), Chapron et al. (2016) used data and published information from instrumented wolves (VHF/GPS). The simulation approach relies on the assumption that instrumented animals were a representative sample of the population, which might not always be the case (Schmidt et al. 2015, Borg et al. 2016). By contrast, our methodology does not rely on simulations, but estimates demographic parameters and their temporal variation from NGS and dead recovery data directly while controlling for spatio-temporal heterogeneity in detection of both live individuals and deaths. As the coverage of DNA samples and dead recoveries extends across nearly all of the Scandinavian wolf population range, the OPSCR model produces population and landscape-level estimates.

Social dynamics. Whereas Chapron et al. (2016) modelled social dynamics explicitly, we did not account for these processes in our model. Wolves are a social species, which violates the assumption of independence between individuals in SCR models. However, using simulations, we confirmed that ignoring non-independence in the spatial distribution and detection patterns of pack members does not lead to noticeable bias in population size or density estimates in social species (RovQuant, unpublished results), consistent with findings reported previously (López-Bao et al. 2018). Any potential issues with spatial non-independence are further mitigated in our model through the inclusion of a spatial covariate on density. Finally, our OPSCR model did distinguish between individuals that had not yet been identified as scent marking members of a pair or pack *vs.* those individuals that had. This allowed us to take into account differences in vital rates and detection probabilities associated with social status. Not surprisingly, given the monitoring focus on packs, pairs and reproductions, and the scent-marking behavior of those individuals, the OPSCR model estimated a higher baseline detection probability for individuals that had at least once been designated as scent-marking members of a pair or pack (Appendix 7, Figure A7.6).

Spatial component. The model that led to CF2 is not spatially explicit, but abundance, detectability, and presumably the demographic structure of the Scandinavian wolf population vary across space. The ability to use spatial information and make spatially explicit predictions (*e.g.* link an abundance estimate with a certain region) is a primary reason for the growing popularity of SCR models in wildlife ecology (Royle et al. 2017). The Scandinavian large carnivore monitoring program is inadvertently configured to make use of this flexible new method. Finally, wolf management in Scandinavia is

inherently spatially explicit, thus clearly benefiting from spatially explicit abundance estimates at user-specified scales (Figure 13; Appendix 7, Table A7.2).

Time-dependent vital rates. The analysis by Chapron et al. (2016) allowed for variation in demographic parameters over time only to a limited degree. For example, mortality due to legal culling was informed by annual dead recoveries, but all other mortalities were assumed to remain constant across years. Yet, there is evidence that vital rates (specifically survival) may vary to a larger extent over time (Milleret 2016), which is bound to have consequences for the ability of a model to predict population size reliably. Our model allowed both sources of mortality to vary across years and the resulting estimates confirmed that there is indeed inter-annual variation in mortality due to legal culling as well as other causes (Appendix 7, A7.7). Annual variation in recruitment was similarly pronounced (Appendix 7, Figure A7.8).

4.2. Search effort, detection probability, and precision

During monitoring seasons 2016/17 and 2017/18, the Swedish EPA decided upon and financed an increased sampling effort. In 2016/17, this entailed an increase in the proportion of collected samples that were subjected to DNA-analysis to 100% (from approximately 50% during previous seasons), without a substantial change in search effort. In 2017/18, search effort increased and became more evenly spread followed by DNA analysis of 100% of the collected samples. The primary goal of this change was to a) collect more DNA samples and achieve greater spatial coverage, thereby increasing the number of detectors (grid cells at which individuals could be detected) and b) increasing the detection probability of all individuals (*i.e.* not focusing solely on pairs and packs), including pups, subadults, vagrants, and solitary territorial animals. This increased effort and scope of the inventory had a direct effect on the baseline detection probability that rose drastically from 2015/16 to 2016/17 and again in 2017/18 (Appendix7). The increased detection probability, in turn, led to noticeably higher precision of key parameter estimates, including population size (narrower credible intervals after the 2015/16 season in Figure 12). The collection pattern during the 2017/18 monitoring season matches the observation process in our model more closely than collections during the previous four monitoring seasons. Prior to that season, monitoring (especially in Sweden) was almost entirely focused on detecting territorial pairs, packs and reproductions, and may have been stopped once sufficient information was collected. DNA presence of pups is not required to determine whether a reproduction has occurred, because the presence of pups and subadults can also be confirmed solely by snow tracking. This limits the probability of genetically detecting individuals that are not scent marking (*e.g.* pups, subadult, vagrant) which can make up about 50% of the total number of individuals present in the population (Chapron et al 2016).

There is an inherent tradeoff between sampling effort and the precision of population size estimates: higher effort leads to a greater number of samples available for analysis, which in turn reduces uncertainty in model estimates. Scandinavian managers may not be able to maintain the 2017/18-level of collection effort during future monitoring seasons, hence an assessment of the relationship between monitoring intensity (*i.e.* number of samples collected and analyzed) and the precision of the population size estimated would be useful to identify an acceptable level of effort. Preliminary results using the 2017/18 season as an example, show that a 25% to 50% reduction in the number of samples collected (or DNA-analyzed) resulted in only moderate decrease in precision and negligible changes in

the point estimate of population size (Figure 18). A more comprehensive evaluation of alternative sampling strategies and their consequences for the precision of population size estimates is currently being performed as part of project RovQuant. This includes exploring the effects of a) a reduction in the number of samples available for analysis (*e.g.* by reducing the number or length of search trails) and b) a decrease in the frequency of monitoring seasons (*e.g.* a reduction from annual to once every 2 or 3 years). Results from this analysis will be available in autumn 2019.

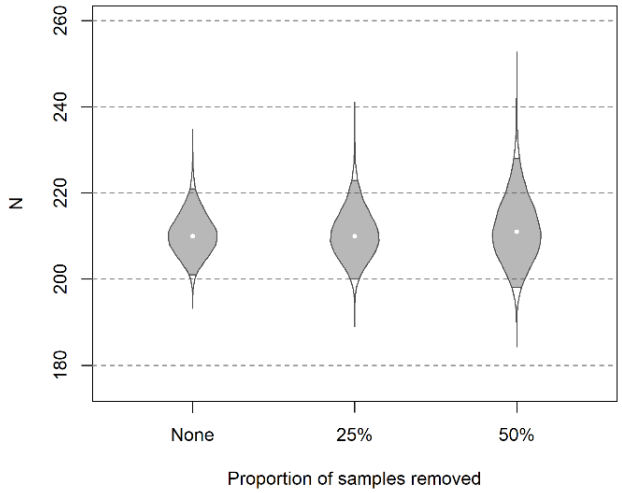

Figure 18. The effect of reduced sampling intensity on population size estimates and associated uncertainty, using the 2017/18 wolf monitoring season as an example. Violins show the OPSCR-estimated number of female wolves in Scandinavia with the original number of samples (left) and random removal of 25% and 50% of samples before model fitting. The estimates presented are from an OPSCR model fitted to only three years of data and include the buffer around the study area.

4.3. Direct *vs.* indirect estimation of population size

Monitoring free-ranging populations is challenging and expensive, for this reason monitoring programs sometimes use counts of population segments that are more readily detected or other indirect indices that can reveal population trends (Knight et al., 1995; Morellet et al., 2007). In combination with conversion factors, such indices can be used to derive population size. Examples are derived population size estimates for Eurasian lynx (*Lynx lynx*) from the number of observed family groups in Scandinavia (Andrén et al. 2002) and South African fur seal (*Arctocephalus pusillus*) from the number of observed pups (Wickens and Shelton 1992).

Several conclusions from this study should be taken into account when considering continued reliance on a conversion factor to derive wolf population size from the number of detected pairs or packs. First, population size is directly estimable from available NGS and dead recovery data. The model described and tested here should be readily applicable to wolf monitoring data during coming years, as long as the collection process (NGS) does not change substantially from the protocol employed in 2017/18. Additionally, we expect model performance (precision and accuracy of the annual population size estimates) to improve as additional years are incorporated into the analysis and the time series lengthens.

Second, the reliability of the conversion factor will depend on annual variation in the population size estimate and the proportion of packs in the population. High human-caused mortality in the

Scandinavian wolf population is one reason for expecting population structure to fluctuate over time and across space. During the five years included in our analysis, the annual conversion factor ranged from 8.6 (CrI: 8.0 - 9.2) to 9.8 (CrI: 9.6 - 10.1) individuals in the population per detected pack. The monitoring bout (2017/18) with the highest conversion factor coincides with a shift to a more comprehensive coverage of the various social and demographic classes in the population during NGS collection. It is thus possible that annual variation we observed in CF3 is a methodological artifact, although our model accounted for temporal and spatial heterogeneity in detection probability. In addition, the elevated conversion factor also coincides with a drop in the number of packs detected, whereas OPSCR-estimated population size remained constant and the number of detected pairs increased between 2016/17 and 2017/18).

Third, the number of detected packs is fraught with imperfect detection. Even though detection of packs is high, some packs may be missed or their status misidentified. Regardless of how precise and trustworthy the abundance estimate underlying the conversion factor is – variation and inaccuracy in the number of packs will lead to bias in the predicted population size. Similarly, imprecisions or potential bias in the population size estimates used to calculate the conversion factor could cause the latter to be unreliable, despite a stable proportion of detected packs.

When economically and logistically feasible, we recommend use of direct means for estimating population size when assessing the status of wolves in Scandinavia and evaluating the impact of management interventions. This is preferable over the use of proxies, such as the number of detected packs in combination with a conversion factor. Within the context of the Scandinavian wolf monitoring and management, a transition to direct population size estimation would entail a shift from pack and pair-centered monitoring to a setup where effort is more evenly spread to detect individuals in the population regardless of demographic and social class. Whether such a shift is feasible will depend on whether less selective (more “even”) monitoring can be accomplished without considerable additional expense and whether it allows monitoring other population parameters that are of interest to managers (number of territories, social status, inbreeding and immigration). Results from a preliminary analysis suggest that precise population size estimates are achievable even with a substantially reduced collection effort compared with the 2017/18 monitoring season (Figure 18). We note that implementation of a modified sample collection protocol tailored to OPSCR-based analysis of the monitoring data does not preclude the continued collection of information about pairs, packs, and social status. Furthermore, a larger proportion of the population sampled, even if this means fewer samples per individual, may also benefit the monitoring of other attributes, such as inbreeding and immigration. The synergistic effect of a more evenly spread search effort for wolf samples will also benefit the monitoring of reproductions of Eurasian lynx (*Lynx lynx*) and wolverine (*Gulo gulo*) NGS sampling in these parts of Scandinavia.

4.4. Recommendations for Scandinavian wolf monitoring

Based on our findings, and if the OPSCR model is to be used for wolf population estimation in the future, we recommend that wolf monitoring continues following the sample collection strategy used during 2017/18. Should maintaining that level of effort prove to not be economically feasible, then we recommend deploying a similar, but lower intensity strategy that continues to give all individuals in the population a chance of being detected at multiple locations. Individuals that are not scent-marking

(*e.g.* pups, sub adult, vagrant) constitute the majority of the population (Chapron et al. 2016). It is therefore essential for reliable estimation of population size with a model like the OPSCR that this segment of the population also be sampled, rather than focusing almost exclusively on pairs and packs. If OPSCR models are to be used to estimate population size in the future, a strategy whereby genetic testing priority is altered based on previous identification should be avoided as it reduces tractability of the observation process in the model. More specifically, we recommend:

1. Continue with population-level monitoring, *i.e.* coordinated sample collection (timing and methods) and data compilation between Norway and Sweden.
2. Implement searches in a manner that gives all individuals present in the population a chance of being detected, without exclusive focus on certain demographic or social classes.
3. Use a regular search grid made up of 5x5 km cells and attempt to search as many cells as possible. Prioritize searching many areas (detector grid cells) over searching fewer sites more intensely to facilitate spatially separated detections.
4. Attempt to search each grid cell at least twice during each monitoring season, with searches separated by at least one week.
5. Collect all sources of DNA found while searching within a cell, unless a sample is clearly attributable to an individual already detected in that cell.
6. If there is a need for sub-selecting samples for DNA analysis, take a random sample of all DNA collected, not a systematic sample based on priority individuals or areas. If subsampling for DNA analysis is not random, record the subsampling scheme so it can be accounted for in the model.
7. Continue recording search effort through track logs.
8. Determine genotype and age of all dead recoveries to improve the precision of the estimates.

In addition, we suggest that authorities evaluate whether a shortened, more intense, monitoring period (*e.g.* December 1 to March 31) would increase synchrony of the sample collection across the monitoring region and lead to less ambiguity about the temporal reference point for population size estimates.

4.5. Further development

Although an effective and flexible tool, the OPSCR model described here has its limitations, including the need to adjust future NGS protocols to more closely resemble those deployed during the 2017/18 season. In order for managers to decide whether this is a feasible strategy for long-term monitoring, a more detailed study using existing data should explore the tradeoff between sampling effort and precision of the parameter estimates. This would help identify survey configurations and levels of search intensity (*e.g.* search track length, proportion of grid cells searched, *etc*.) that would produce estimates with a desired precision.

In terms of technical developments, incorporating age structure and group dynamics/sociality in the model would provide more detailed information about population dynamics and allow direct estimation of the number of packs and pairs (including uncertainty). This would also allow quantifying inter annual variation in population structure (which affects the conversion factor) and identify mechanisms driving it. Additionally, goodness-of-fit methods for OPSCR models are still in their infancy and should be further developed in order to help identify potential model misspecifications.

Finally, vital rates and the composition of the population are liable to vary not only through time but also across space. This variation should be estimated as it may have consequences for local management and could help identify hotspots and guide management interventions (*e.g.* areas with high levels of undetected mortality).

Like all scientific work, the contents of this report should be subjected to rigorous peer review before its conclusions and recommendations are adopted within an adaptive management framework and converted into policy. We intend to compile the information presented here in a scientific article for submission to an international, peer-reviewed journal during 2019. Numbers provided in this report may change in subsequent publications, as models are improved and additional years of data are incorporated.

5. Acknowledgements

We thank L. Svensson, A. Ordiz, G. Chapron, and J. Vermaat for helpful comments on drafts of this report, O. Gimenez for methodological advice, and P. de Valpine and D. Turek for assistance with the formulation of the OPSCR model in Nimble. This work would not have been possible without the monitoring data collected by Swedish (Länstyrelsen) and Norwegian (SNO) wildlife management authorities, as well as the public in both countries. Similarly, this work relied on genetic analyses conducted by the laboratory personnel at the DNA laboratories at Grimsö Wildlife Research station, Sweden and at the Norwegian Institute for Nature Research, Norway. We also thank Swedish and Norwegian wildlife managers for feedback they provided during the RovQuant workshop in June 2018 and the Swedish-Norwegian carnivore management meeting in December 2018. The study was funded primarily by Naturvårdsverket, with additional funding from Miljødirektoratet to project RovQuant. Computation support was provided by NMBU's computing cluster "Orion", administered by the Centre for Integrative Genetics.

6. References

Åkesson, M., A. Danielsson, E. Hedmark, and F. Öhrn. 2018. Teknisk rapport över genetiska analyser på varg i Sverige år 2017. Rapport från SLU.

Åkesson, M., O. Liberg, H. Sand, P. Wabakken, S. Bensch, and Ø. Flagstad. 2016. Genetic rescue in a severely inbred wolf population. Molecular Ecology 25:4745–4756.

Åkesson, M., and L. Svensson. 2018. Sammanställning av släktträdet över den skandinaviska vargpopulationen fram till 2017. Rapport från Viltskadecenter, SLU 2018-3.

Alfredèen, A.-C. 2006. Denning behaviour and movement pattern during summer of wolves Canis lupus on the Scandinavian Peninsula. Grimsö forskningsstation SLU.

Andrén, H., J. D. C. Linnell, O. Liberg, P. Ahlqvist, R. Andersen, A. Danell, R. Franzén, T. Kvam, J. Odden, and P. Segerström. 2002. Estimating total lynx *Lynx lynx* population size from censuses of family groups. Wildlife Biology 8:299–306.

Bischof, R., H. Brøseth, and O. Gimenez. 2016. Wildlife in a Politically Divided World: Insularism Inflates Estimates of Brown Bear Abundance. Conservation Letters 9:122–130.

Bischof, R., P. Dupont, C. Milleret, H. Brøseth, J. Chipperfield, O. Gimenez, A. Ordiz, M. Tourani, and J. Kindberg. 2017. Project RovQuant Integrated analysis using data from Rovbase 3.0 to guide adaptive management of large carnivores in Norway and Sweden. Report 2017.1 of the Applied Quantitative Ecology Group (AQEG) to the Norwegian Environment Agency (Miljødirektoratet).

Bischof, R., J. E. Swenson, N. G. Yoccoz, A. Mysterud, and O. Gimenez. 2009. The magnitude and selectivity of natural and multiple anthropogenic mortality causes in hunted brown bears. Journal of Animal Ecology 78:656–665.

Borg, B. L., S. M. Arthur, N. A. Bromen, K. A. Cassidy, R. McIntyre, D. W. Smith, and L. R. Prugh. 2016. Implications of Harvest on the Boundaries of Protected Areas for Large Carnivore Viewing Opportunities. PLOS ONE 11:e0153808.

Chapron, G., C. Wikenros, O. Liberg, P. Wabakken, Ø. Flagstad, C. Milleret, J. Månsson, L. Svensson, B. Zimmermann, M. Åkesson, and H. Sand. 2016. Estimating wolf (Canis lupus) population size from number of packs and an individual based model. Ecological Modelling 339:33–44.

Dupont, P., C. Milleret, O. Gimenez, and R. Bischof. 2019. Population closure and the bias-precision trade-off in spatial capture–recapture. Methods in Ecology and Evolution 0:1–12.

Efford, M. G. 2011. Estimation of population density by spatially explicit capture-recapture analysis of data from area searches. Ecology 92:2202–2207.

Ergon, T., and B. Gardner. 2014. Separating mortality and emigration: modelling space use, dispersal and survival with robust-design spatial capture–recapture data. Methods in Ecology and Evolution 5:1327–1336.

Gardner, B., R. Sollmann, N. S. Kumar, D. Jathanna, and K. U. Karanth. 2018. State space and movement specification in open population spatial capture-recapture models. Ecology and Evolution 0.

Gelman, A. 1996. Inference and monitoring convergence. Pages 131–143 *in* W. R. Gilks, S. Richardson, and D. J. Spiegelhalter, editors. Markov chain Monte Carlo in practice. Chapman and Hall, London, UK.

Gelman, A., and C. R. Shalizi. 2013. Philosophy and the practice of Bayesian statistics. British Journal of Mathematical and Statistical Psychology 66:8–38.

Liberg, O., H. Andrén, H.-C. Pedersen, H. Sand, D. Sejberg, P. Wabakken, M. Kesson, and S. Bensch. 2005. Severe inbreeding depression in a wild wolf (Canis lupus) population. Biology letters 1:17–20.

Liberg, O., Å. Aronson, H. Sand, P. Wabakken, E. Maartmann, L. Svensson, and M. Åkesson. 2012. Monitoring of wolves in Scandinavia. Hystrix, the Italian Journal of Mammalogy 23:29–34.

Liberg, O., G. Chapron, P. Wabakken, H. C. Pedersen, N. T. Hobbs, and H. Sand. 2011. Shoot, shovel and shut up: cryptic poaching slows restoration of a large carnivore in Europe. Proceedings of the Royal Society B: Biological Sciences 279:910–915.

López-Bao, J. V, R. Godinho, C. Pacheco, F. J. Lema, E. García, L. Llaneza, V. Palacios, and J. Jiménez. 2018. Toward reliable population estimates of wolves by combining spatial capture-recapture models and non-invasive DNA monitoring. Scientific reports 8:2177.

Milleret, C. 2016. Spatial ecology of wolves in Scandinavia: From spatio-temporal dynamics of wolf pairs to wolf population dynamics. PhD Thesis.

Milleret, C., P. Dupont, C. Bonenfant, H. Brøseth, Ø. Flagstad, C. Sutherland, and R. Bischof. 2018a. A local evaluation of the individual state-space to scale up Bayesian spatial capture-recapture. Ecology and evolution 9:352–363.

Milleret, C., P. Dupont, H. Brøseth, J. Kindberg, J. A. Royle, and R. Bischof. 2018b. Using partial aggregation in spatial capture recapture. Methods in Ecology and Evolution 9:1896–1907.

Milleret, C., P. Wabakken, O. Liberg, M. Akesson, O. Flagstad, H. P. Andreassen, and H. Sand. 2016. Let's stay together? Intrinsic and extrinsic factors involved in pair bond dissolution in a recolonizing wolf population. Journal of Animal Ecology 86.

NIMBLE Development Team. 2019. NIMBLE: MCMC, Particle Filtering, and Programmable Hierarchical Modeling. https://cran.r-project.org/package=nimble.

Nonaka, Y. 2011. Response of breeding wolves to human disturbance on den sites. Master's thesis, Uppsala University.

Ordiz, A., C. Milleret, J. Kindberg, J. Månsson, P. Wabakken, J. E. Swenson, and H. Sand. 2015. Wolves, people, and brown bears influence the expansion of the recolonizing wolf population in Scandinavia. Ecosphere 6:1–14.

Plummer, M. 2003. JAGS: A program for analysis of Bayesian graphical models using Gibbs sampling. Page Proceedings of the 3rd International Workshop on Distributed Statistical Computing (DSC 2003), March 20–22. Vienna, Austria.

R Core Team. 2018. R: A language and environment for statistical computing. R Foundation for Statistical Computing, Vienna, Austria. https://www.R-project.org/.

Royle, J. A., R. B. Chandler, R. Sollmann, and B. Gardner. 2013. Spatial capture-recapture. Elsevier/Academic Press, Amsterdam.

Royle, J. A., R. M. Dorazio, and Link W.A. 2007. Analysis of multinomial models with unknown index using data augmentation. Journal of Computational and Graphical Statistics 16(1):67–85.

Royle, J. A., A. K. Fuller, and C. Sutherland. 2017. Unifying Population and Landscape Ecology with Spatial Capture-recapture. Ecography 41:444–456.

Royle, J. A., K. U. Karanth, A. M. Gopalaswamy, and N. S. Kumar. 2009. Bayesian inference in camera trapping studies for a class of spatial capture–recapture models. Ecology 90:3233–3244.

Sanz-Pérez, A., A. Ordiz, H. Sand, J. E. Swenson, P. Wabakken, C. Wikenros, B. Zimmermann, M. Åkesson, and C. Milleret. 2018. No place like home? A test of the natal habitat-biased dispersal hypothesis in Scandinavian wolves. Royal Society Open Science 5:181379.

Schmidt, J. H., D. S. Johnson, M. S. Lindberg, and L. G. Adams. 2015. Estimating demographic parameters using a combination of known-fate and open N-mixture models. Ecology 96:2583–2589.

Svensson, L., P. Wabakken, I. Kojola, E. Maartmann, T. Strømseth, M. Åkesson, and Ø. Flagstad. 2014. Varg i Skandinavien och Finland: Slutrapport fraøninventering av varg vintern 2013–2014. Høgskolan i Hedmark.

Svensson, L., P. Wabakken, E. Maartmann, M. Åkesson, and Ø. Flagstad. 2015. Inventering av varg vintern 2014-2015. Inventeringsresultat för stora rovdjur i Skandinavien 1-2015.

Svensson, L., P. Wabakken, E. Maartmann, M. Åkesson, and Ø. Flagstad. 2017. Inventering av varg vintern 2016-2017 / Bestandsovervåking av ulv vinteren 2016-2017. Page Bestandsstatus for store rovdyr i Skandinavia.

Svensson, L., P. Wabakken, E. Maartmann, M. Åkesson, and Ø. Flagstad. 2018. Bestandsovervåking av ulv vinteren 2017-2018 / Inventering av varg vintern 2017-2018. Page Bestandsstatus for store rovdyr i Skandinavia.

Turek, D., P. de Valpine, and C. J. Paciorek. 2016. Efficient Markov chain Monte Carlo sampling for hierarchical hidden Markov models. Environmental and Ecological Statistics 23:549–564.

de Valpine, P., D. Turek, C. J. Paciorek, C. Anderson-Bergman, D. T. Lang, and R. Bodik. 2017. Programming With Models: Writing Statistical Algorithms for General Model Structures With NIMBLE. Journal of Computational and Graphical Statistics 26:403–413.

Vilà, C., A. Sundqvist, Ø. Flagstad, J. Seddon, S. Björnerfeldt, I. Kojola, A. Casulli, H. Sand, W. Petter, and E. Hans. 2003. Rescue of a severely bottlenecked wolf (Canis lupus) population by a single immigrant. Proceedings of the Royal Society of London. Series B: Biological Sciences 270:91–97.

Wabakken, P., Å. Aronson, H. Sand, H. Rønning, and I. Kojola. 2004. Ulv i Skandinavia. Statusrapport for vinteren 2002-2003. Høgskolen i Hedmark, Viltskadecenter, Grimsö forskningsstation, Vilt- og fiskeriforskningen, Oulu. Høgskolen i Hedmark Oppdragsrapport 2.

Wabakken, P., Å. Aronson, H. Sand, Steinset, O.K., and I. Kojola. 2001a. Ulv i Skandinavia. Statusrapport for vinteren 2000-2001. Høgskolen i Hedmark, Viltskadecenter, Grimsö forskningsstation, Vilt- og fiskeriforskningen, Oulu. Høgskolen i Hedmark. Oppdragsrapport 1.

Wabakken, P., Å. Aronson, H. Sand, Steinset, O.K., and I. Kojola. 2002. Ulv i Skandinavia. Statusrapport for vinteren 2001-2002. Høgskolen i Hedmark, Viltskadecenter, Grimsö forskningsstation, Vilt- og fiskeriforskningen, Oulu. Høgskolen i Hedmark Oppdragsrapport 2.

Wabakken, P., H. Sand, O. Liberg, and A. Bjärvall. 2001b. The recovery, distribution, and population dynamics of wolves on the Scandinavian peninsula, 1978-1998. Canadian Journal of Zoology 79:710–725.

Wabakken, P., L. Svensson, E. Maartmann, M. Åkesson, and Ø. Flagstad. 2016. Bestandsovervåking av ulv vinteren 2015-2016. Page Bestandsstatus for store rovdyr i Skandinavia.

Wickens, P. A., and P. A. Shelton. 1992. Seal pup counts as indicators of population size. South African Journal of Wildlife Research Number 3, 1 January 1992, pp. 65-69(5) 22:65–69.

Williams, B. K., J. D. Nichols, and M. J. Conroy. 2002. Analysis and management of animal populations. Academic Press, San Diego, California, USA.

Appendices

1 – 7

Table of Contents

Appendix 1. Description of the original conversion factor (CF1) 51
Appendix 2. Input data 53
Appendix 3. OPSCR model description 57
Appendix 4. Table of priors used for OPSCR model parameters 63
Appendix 5. OPSCR model simulation test 65
Appendix 6. Bayesian posterior predictive checks 69
Appendix 7. Parameter estimates 71

Appendix 1. Description of the original conversion factor (CF1)

During the work presented in this report, we have found it challenging to track down a detailed and reproducible description of the calculation of the uncertainty associated with the original conversion factor (CF1) and how it is used to derive 95% confidence limits of population size estimates. For this reason, we provide here a description of the process, based chiefly on a compilation of information in existing reports (Wabakken et al. 2001, 2002, 2004, Svensson et al. 2014) and a document ("2019-02-05 description present conversion factor.docx") and data file ("Population estimate-2017-2018-PW-20180531.xls") provided by the Scandinavian Wolf Project (Skandulv) to the Swedish environmental protection agency (Naturvårdsverket; J. Andersson pers. comm. 2019-02-28).

CF1 is based on the following empirical information collected during monitoring seasons 2000/01, 2001/02, and 2002/03 (Wabakken et al. 2001, 2002, 2004).

- annual counts of the detected number of reproductions (see Box 1 in the main text)
- minimum and maximum number of detected wolves

The following steps were taken to calculate the overall conversion factor between the number of detected reproductions and total population size (Svensson et al. 2014):

1. Calculate a minimum and maximum conversion factor for each year by dividing the annual minimum and maximum number of wolves reported to have been present by the number of reproductions reported during the respective monitoring period.
2. Take the annual average of the minimum and maximum conversion factors calculated in step 1.
3. Take the average of the three annual conversion factors calculated in step 2. This yields an average conversion factor of 10.

The average of the three annual minimum conversion factors was presented as the lower uncertainty boundary (9.3 individuals per reproduction) around CF1. Similarly, the average of the three annual maximum conversion factors was presented as the upper uncertainty boundary (10.7 individuals per reproduction) around CF1. Note that based on the data provided in table 2 in Svensson et al. (2014), the actual average of the 3 annual maximum conversion factors is 10.6 and not 10.7. We have not been able to find an explanation for the discrepancy between the calculated and reported upper uncertainty boundary.

Although the aforementioned uncertainty boundaries (9.3-10.7) are provided in publications related to CF1 (e.g. Svensson et al. 2014, Chapron et al. 2016), starting in 2014, uncertainty boundaries around the CF1-derived population size estimates were calculated using different conversion factor values. These are 7.9 and 13 individuals per reproduction, respectively leading to the reported lower and upper so-called 95% confidence interval (referred as "pseudo-95% confidence interval" in Chapron et al. 2015) around the population size estimates reported by the monitoring program (Wabakken et al. 2016, Svensson et al.

2017, 2018). These lower and upper conversion factor values were calculated as follows (according to the file “Population estimate-2017-2018-PW-20180531.xls” provided by Skandulv to Naturvårdsverket):

1. Calculate mean and standard deviation of the 3 annual minimum conversion factors, then use the formulae mean - 4.303se to obtain the lower 95% CI (7.9 individuals per reproduction) associated with the 3 annual minimum conversion factors.
2. Calculate the mean and standard deviation of the 3 annual maximum conversion factors, then use the formulae mean + 4.303se to obtain the upper 95% CI (13 individuals per reproduction) associated with the 3 annual maximum conversion factors.

The formula used to derive the 95% confidence limits ($mean \pm 4.303sd/\sqrt{n}$) from only n=3 data points (three annual minimums and three annual maximums) is based on the 95% quantile of a Student’s t distribution with 2 degrees of freedom. This amounts to a computation of separate 95% confidence intervals (not valid if the underlying distribution differs from the Normal distribution) on both the minimum and maximum counts, which should not be interpreted as 95% CIs around the population size estimates.

Appendix 2. Input data

Table A2.1 Number of samples collected during the winter monitoring period (October 1 – March 31) in Scandinavia from 2013-2017. Number of samples are reported for Males (M) and Females (F) in Norway and Sweden.

	2013		2014		2015		2016		2017		TOTAL
	M	F	M	F	M	F	M	F	M	F	
Norway	65	47	100	92	172	145	195	259	276	268	1619
Sweden	228	180	221	173	364	235	1102	835	1470	1051	5859
TOTAL	293	227	321	265	536	380	1297	1094	1746	1319	7478

Table A2.2 Number of individuals detected via NGS during the winter monitoring period (October 1 – March 31) from 2013-2017. Number of detected individuals are reported for Males (M) and Females (F) in Norway and Sweden. Some individuals were detected in both countries during the same year.

	2013		2014		2015		2016		2017		TOTAL
	M	F	M	F	M	F	M	F	M	F	
Norway	22	17	31	28	42	30	35	46	46	49	**346**
Sweden	102	84	95	87	124	90	154	139	156	143	**1174**

Table A2.3 Number of cause-specific dead recoveries in Scandinavia from 2013-2017. Number of dead recoveries are reported for Males (M) and Females (F) in Norway and Sweden.

Cause	Country	2013		2014		2015		2016		2017		Total
		M	F	M	F	M	F	M	F	M	F	
Other	Norway	3	1	0	0	2	1	0	0	0	1	**8**
	Sweden	5	4	11	7	5	7	2	4	0	2	**47**
Legal culling	Norway	7	5	8	4	6	6	7	7	11	16	**77**
	Sweden	10	11	32	33	20	8	26	20	28	15	**203**
	TOTAL	**25**	**21**	**51**	**44**	**33**	**22**	**35**	**31**	**39**	**34**	**335**

Table A2.4 Number of detected packs, scent-marking pairs and reproductions in Sweden, Norway and across the border from 2013-2017 (from Svensson et al. 2014, 2015, 2017, 2018, Wabakken et al. 2016)

Year	Number of pairs				Number of packs				Number of reproductions			
	Total	**S**	**N**	**Border**	**Total**	**S**	**N**	**Border**	**Total**	**S**	**N**	**Border**
2013	23-24	19	2-3	2	43	35	3	5	40	32	3	5
2014	19	11	3	5	49	41	3	5	46	39	2	5
2015	29	24	4	1	41	30	7	4	43	32	4	7
2016	28	19	6	3	46	34	5	7	43	32	4	7
2017	31	23	3	5	41	28	8	5	41	28	8	5

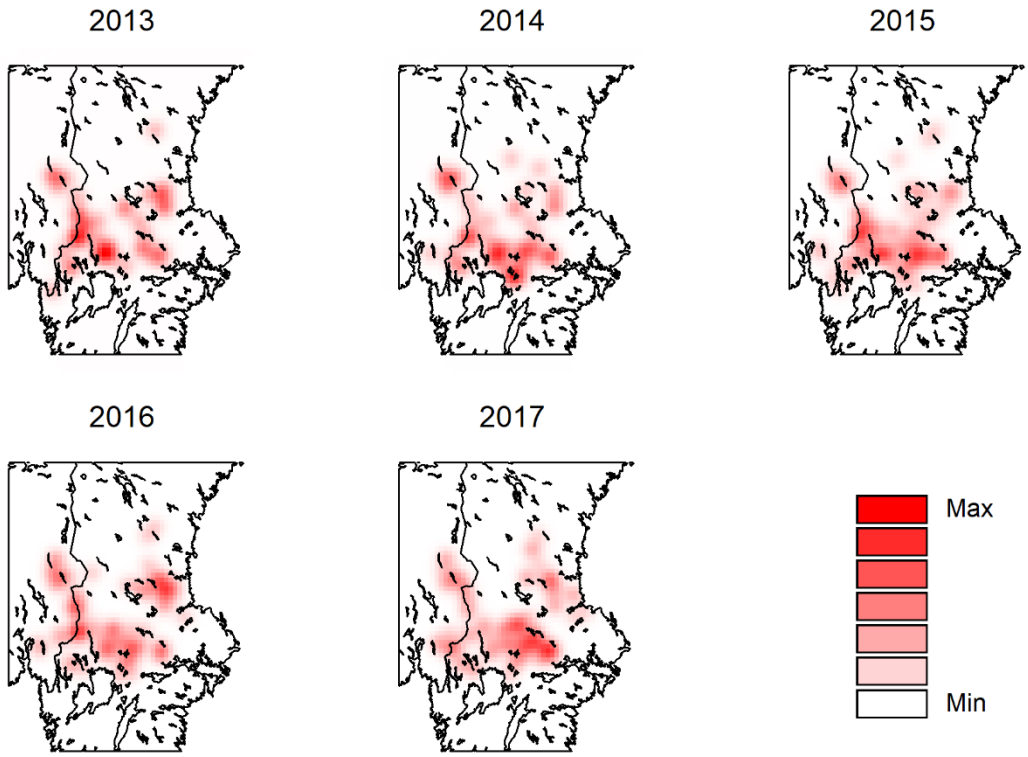

Figure A2.5. *Maps of the relative annual density of detected wolf packs. Relative density was estimated with a kernel utilization distribution from the detection locations of wolf packs. This variable was used as a covariate shaping the intensity surface in the point process sub-model of the OPSCR model (for AC locations placement and movement).*

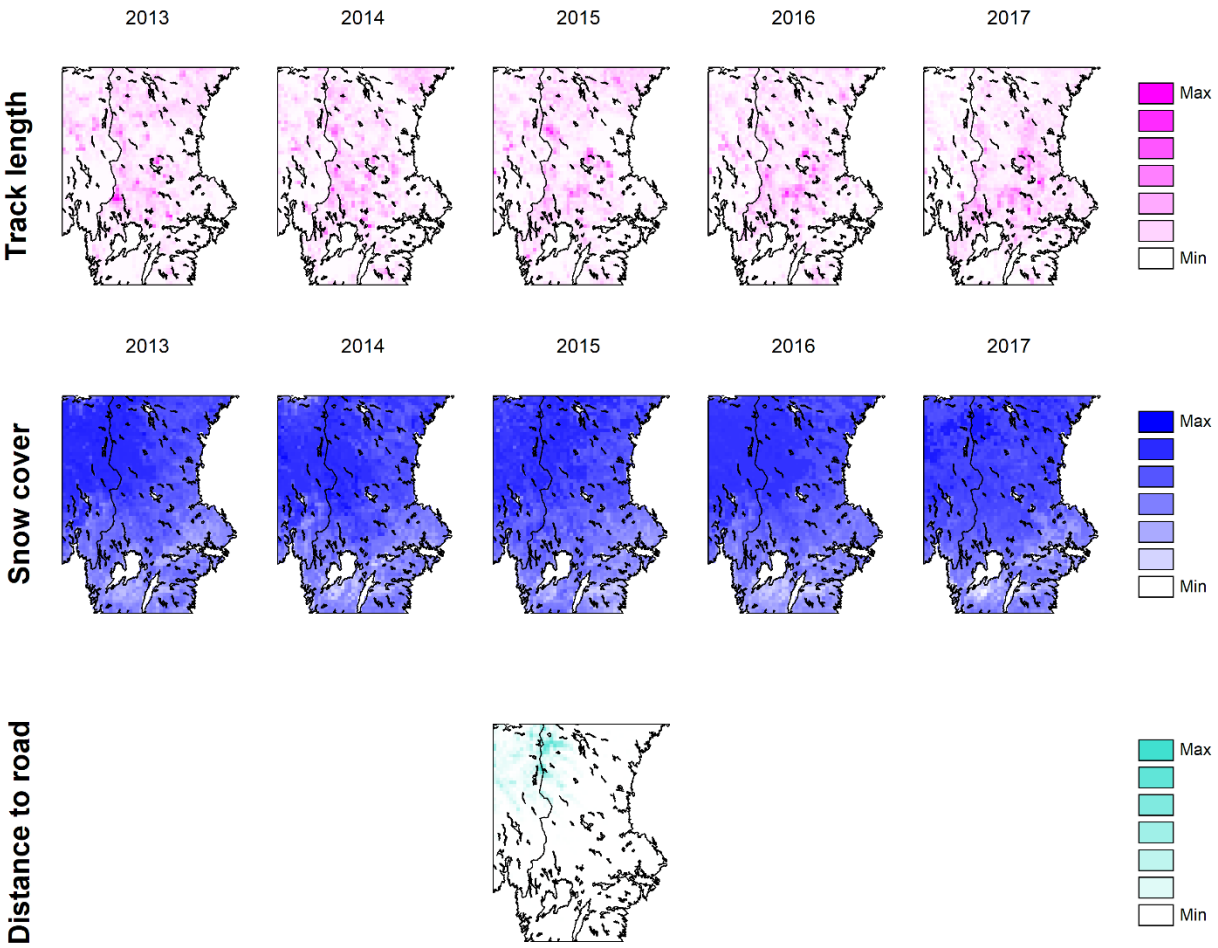

Figure A2.6. *Spatial covariates used on the baseline detection probability. The length of search tracks and proportion of snow cover (MODIS, https://neo.sci.gsfc.nasa.gov, accessed the 12/14/2018 obtained on a monthly basis at 0.1 degrees resolution) vary between years, whereas distance to road is constant across time. All variables were standardized for analysis.*

Appendix 3. OPSCR model description

General information

We built a Bayesian open-population spatial capture recapture (OPSCR) model that contained three main components:

1) A point process model that describes the placement of individual AC locations each year as well as the movement of these ACs between years (Ergon and Gardner 2014).
2) A multistate demographic model that describes the transitions of individuals between demographic states from year to year (*e.g.* recruitment, survival/mortality; Seber 1965, Schwarz and Arnason 1996).
3) A detection model that describes the probability to detect (or miss) individuals in the population in a spatially explicit manner, based on their latent AC location and different spatial covariates (*e.g.* snow cover, distance to roads, tracking effort).

Our OPSCR model is based on the same core elements as more classical SCR models. SCR models are hierarchical state-space models combining 1) a point process model that describes the spatial distribution of individual ACs, and 2) a detection model, conditional on the point process model, which describes the relationship between individual detection probability and distance to its AC. The standard half-normal detection model used in SCR assumes that the probability *p* of detecting individual *i* at detector *j* and time *t* decreases with distance between the detector and the AC (D_{ijt}):

$$p_{ijt} = p_{0_{ijt}}.e^{-\frac{D_{ijt}^2}{2\sigma^2}}$$

where $p_{0_{ijt}}$ represents the baseline detection probability at the location of the AC, and σ, the scale parameter, represents the width of the detection distribution. The scale parameter σ is related to the extent of space used over the period of study.

In SCR, the locations of ACs (s_{it}) are generally modelled as a homogenous point process that assumes that s_{it} are uniformly distributed across the spatial domain (S; but see section 3.4 for our development and application of an inhomogeneous point process model). In OPSCR models, ACs can shift position from one year to another (Ergon and Gardner 2014, Gardner et al. 2018).

We used Markov Chain Monte Carlo (MCMC) simulation and data augmentation to analyze SCR models and obtain estimates of abundance (Royle et al. 2007, 2009). Data augmentation requires augmenting the dataset with an arbitrary (but sufficiently large) number of individuals that were never detected. We used 0.8 times the total number of individuals detected of all years, as this was proven sufficient in preliminary analyses. It also requires including an associated latent variable *z* reflecting the state of an individual to differentiate between individuals that were present in the population but not detected from individuals that could not be detected, as they were not part of the population (*i.e.* the "unborn" state in our case, see below for definitions of states and state transitions). Estimated abundance ($\widehat{N_t}$) is then derived by summing the number of individuals in alive states, and density *d* is derived by dividing $\widehat{N_t}$ by the area of S.

Details of the spatial capture-recapture model

In order to account for spatio-temporal and individual heterogeneity in detection probability, we modelled $p_{0_{ijt}}$ as

$$logit\left(p_{0_{ijt}}\right) = p0Intercept_{j\,z_{it}t} + \beta_1 * IdResponse_{it} + \beta_2 * DistRoads_j + \beta_3 * Snow_{jt} + \beta_4 * Tracks_{jt}$$

Where $p0Intercept$ is stratified by spatial unit (*e.g.* county), individual state, and year. $IdResponse$ is the covariate representing whether or not (1/0) the individual has been detected during the previous monitoring period. $DistRoads$ is the distance from each detector to the nearest road. $Snow$ represents the average snow cover at each detector (obtained on a monthly basis at 0.1 degrees resolution) during each monitoring period (October 1- April 1; https://neo.sci.gsfc.nasa.gov, accessed the 12/14/2018). $Tracks$ is the total length of GPS tracks within a detector grid cell and in each monitoring period. This covariate represents the intensity of the tracking effort in each detector cell and for each monitoring period (tracking on foot/skis, snow mobile and cars; excluding helicopter flights).

We aggregated all detections to the closest detector using the partially aggregated binomial observation model (Milleret et al. 2018b). The PAB model consists in dividing each detector cell into *K* sub-detector cells and model the frequency of sub-detectors with at least one detection as a binomial response with *K* trials. We defined detectors as the center of all 10 km resolution grid cells covering the study area and sub-detectors as the center of cells that divided these main grid cells in 100 cells (1km resolution). Only sub-detectors that overlapped with the suitable habitat were defined as active and used to calculate the number of trials for detector K_j:

$$y_{ijt} \sim Binomial(p_{ijt}, K_j)$$

Where y is a detection array with the number of detections of individual *i* at detector *j* (number of sub-detectors with at least one detection) and during monitoring period t. Aggregating information with this method decreases the number of detectors and therefore the computational burden. However when too coarse, aggregation can cause severe bias in the estimates of the scale parameter of the detection function. We therefore kept the detector spacing to 10 km, so that it did not exceed 1.5 times *σ (σ≈8km* as revealed from preliminary analyses) as recommended by our previous work (Milleret et al. 2018b).

We assumed fixed AC location during the entire monitoring period. Even if adult wolves are territorial and the monitoring period did not overlap with the main natal dispersal period of the wolf in Scandinavia (Chapron et al. 2016), some individual detections were > 45km apart from each other within a single monitoring period. Assuming a circular home range, this amounts to the size of the largest annual home range size diameter reported for wolves in Scandinavia (approximately 1600km2; Mattisson et al. 2013). Therefore, those detections are more likely to be associated with dispersal than territorial behavior. Although only a few individuals (average of 4.8% of individuals detected each year) and detections (average of 2.1% of the annual number of detections) were concerned, incorporating these detections would prevent the use of the local evaluation of the individual state space (LESS; Milleret et al. 2018a), an efficient approach to reduce the computation burden of large-scale SCR models. We therefore calculated the pairwise Euclidean distances between all detections of

each individual in each monitoring period and discarded detections that were further than 45 km apart while aiming at maximizing the total number of detections retained.

Multistate population dynamic model

Individual state z_{it} takes the value 1 if "unborn", 2 if "alive other", 3 if "alive scent-marking adult", 4 if "dead legal" (newly dead from legal culling), and 5 if "dead" (newly dead from other causes or dead from any cause in a previous time step). z_{it} is modeled as the result of a Markovian process and changes with time according to a categorical distribution describing the transition probabilities from the current state to all other possible states (Gimenez et al. 2007, Kery and Schaub 2011). At the first occasion, individuals can only be designated as "unborn", "alive other" or "alive scent-marking adult" so that $z_{i1} \sim dcat(omeg1[1:3])$, where $omeg1$ follows a Dirichlet distribution such that $omeg1 \sim ddirch(alpha[1:3])$, where alpha is a vector of prior probabilities all equal to 1/3.

For *t≥2*, z_{it} is conditioned on the state of the individual at *t-1:*

- If $z_{it-1} = 1$, the individual can either be recruited (transition to $z_{it} = 2$) or stay in the "unborn" state ($z_{it} = 1$), so that $z_{it} \sim dcat(1 - \gamma_t, \gamma_t, 0, 0, 0)$, where γ_t is a recruitment parameter. This parameter was made time-specific, as it is conditional on the number of individuals that are left in the departure state (*i.e.* the "unborn" state) at time *t*. A per capita recruitment rate can be derived as the number of new recruits *t,* divided by the number of individuals alive at *t-1.*
- If $z_{it-1} = 2$, the individual can either survive and remain in state "alive other" ($z_{it} = 2$), survive but transition to state "alive scent-marking adult" ($z_{it} = 3$), die from legal culling ($z_{it} = 4$), or die from other causes and transition to $z_{it} = 5$. Therefore $z_{it} \sim dcat(0,\ \varphi_{tz_{it-1}}.(1 - \psi_t),\ \varphi_{tz_{it-1}}.\psi_t,\ h_{tz_{it-1}},\ w_{tz_{it-1}})$, where $\varphi_{tz_{it-1}}$ represents the state-specific survival probability, ψ_t the transition probability from state 2 to 3, $h_{tz_{it-1}}$ the state-specific probability of dying from legal culling, and $w_{tz_{it-1}}$ the state-specific probability of dying from other causes (Bischof et al. 2009). Note that $h_{tz_{it-1}} + w_{tz_{it-1}} + \varphi_{tz_{it-1}}$ must be = 1. The fact that state 4 has perfect detectability (all legal deaths are reported), makes w and h identifiable.
- If $z_{it-1} = 3$, the individual can either survive and remain in state "alive scent-marking adult" ($z_{it} = 3$), die from legal culling ($z_{it} = 4$), or die from other causes ($z_{it} = 5$). Therefore. $z_{it} \sim dcat(0,\ 0,\ \varphi_{tz_{it-1}},\ h_{tz_{it-1}},\ w_{tz_{it-1}})$.
- Finally, all individuals in dead states ($z_{i,t-1} = 4$ or 5) transition to $z_{it} = 5$, the absorbing state.

Because only individuals in the live states 2 and 3 can be detected, we conditioned the observation variable y_{ijt} denoting the number of sub-detectors with detections of individual *i* at detector *j* and time *t* on its current individual state z_{it}:

$$y_{ijt} \sim Binomial(p_{ijt} * I(z_{it} = 2 | z_{it} = 3), K_j)$$

where I is an indicator function returning 1 for z = 2 and z = 3, and 0 for individuals in state 1, 4, and 5. Kj is the number of sub-detectors of detector j.

Annual estimates of abundance ($\widehat{N_t}$) were obtained as:

$$\widehat{N}_t = \sum_{i=1}^{M} I(z_{it} = 2 | \, z_{it} = 3)$$

The state z_{it} of an individual is a latent state, except at occasions when the individual was detected alive or recovered dead. In some cases, it is also possible to reconstruct with certainty the state of individuals in years without detections. For example, an individual is known to be alive in years in which it was not detected, if that period is framed by alive detections.

Point process model

During the first occasion (initial year of the study), ACs were placed in the available habitat (*S*) following an inhomogeneous Binomial point process (Illian et al. 2008). This formulation allows the density of activity centers to vary spatially according to a spatial intensity function, $\lambda(\boldsymbol{x})$ (where $\boldsymbol{x}$ is a vector of spatial coordinates). Then, the expected number of activity centers falling within an area *U* (here defined as *D*) follows

$$D \sim Binomial(\frac{\Lambda(U)}{\Lambda(S)}, M)$$

where *M* is the total number of activity centers (including "unborn" individuals) in the entire habitat available (*S*) and

$$\Lambda(U) = \iint_{U} \lambda(\boldsymbol{x}) \, d\boldsymbol{x}$$

In this study, we define the intensity function of the inhomogeneous binomial point process to condition the initial AC locations on the density of known packs the previous year ($PackDensity_0$; see Figure A2.2)

$$\lambda(\boldsymbol{x}) = e^{\beta . PackDensity_0(\boldsymbol{x})}$$

where $PackDensity_0(\boldsymbol{x})$ is the density of known packs at the point with coordinates $\boldsymbol{x}$ and β is the effect of the density of detected packs on the spatial intensity surface.

In order to distinguish between emigration and mortality, we integrated AC movement into the OPSCR model by allowing shifts of individual activity centers between years. This is an important component of the OPSCR model as it can improve survival estimates and can take into account the impact of animals moving within and out of the sampled area (Ergon and Gardner 2014, Gardner et al. 2018). To account for the fact that individual movements are the result of both the attractiveness of the habitat at the arrival location (habitat selection) and the distance from the original location, movement was modelled as a Markovian inhomogeneous binomial point process. This means that we defined the intensity function of the spatial point process such that the placement of an activity center at time *t,* with coordinates $\boldsymbol{x}_t$, conditioned on both the AC location the previous year, with coordinates $\boldsymbol{x}_{t-1}$(Markovian), and on the density of known packs the previous year (inhomogeneous point process description above):

$$\lambda(\boldsymbol{x}_t, \tau, \boldsymbol{x}_{t-1}) = e^{-\frac{d_t^2}{2\tau^2}} * e^{\beta . PackDensity_{t-1}(\boldsymbol{x}_t)}$$

where d_t is the Euclidian distance between the consecutive AC locations and τ is the standard deviation of a bivariate normal distribution centered on $\boldsymbol{x}_{t-1}$. Under this specification, the spatial intensity function describes movement as a series of isotropic Gaussian random walks (see also Gardner et al. 2018) weighted by the density of known packs the previous year. The standard deviation τ therefore regulates the distance that individuals are likely to move between time periods.

Appendix 4. Table of priors used for OPSCR model parameters

Table A4.1 Description, prior distributions, and initial values for parameters estimated by the OPSCR model

Parameter	Description	Prior	Initial values
dispSigma (τ)	Dispersal sigma describing the movement of AC locations between years	dgamma(0.01,0.01)	runif(1,30,70)
beta.dens (β)	Effect of the density of known packs on AC locations.	dnorm(0.0,0.01)	runif(1,-1,1)
h	Mortality probability due to legal culling	dunif(0,1)	runif(1,0.2,0.4)
w	Mortality probability due other causes	dunif(0,1)	runif(1,0.2,0.4)
phi (φ)	Survival probability		*1-h-w*
omeg1	vector of inclusion probabilities during the first year	ddirch(alpha[1:3]) alpha[1:3] <- c(1,1,1)	c(0.5,0.25,0.25)
gamma (γ)	Transition probability from state 1 to state 2	dunif(0,1)	runif(1,0,1)
psi (ψ)	Transition probability from state 2 to state 3 conditional on survival	dunif(0,1)	runif(1,0.1,0.7)
sigma (σ)	Scale parameter of the half-normal detection function	dunif(0,100)	runif(1,5,15)
betaResponse (β_1)	Effect of previous detection of individual on detection probability	dunif(-5,5)	runif(1,-1,1)
betaRoads (β_2)	Effect of distance to the closest roads on detection probability	dunif(-5,5)	runif(1,-1,1)
betaTracks (β_4)	Effect of search-effort (track length) on detection probability	dunif(-5,5)	runif(1,-1,1)
betaSnow (β_3)	Effect of average snow cover during the monitoring period on detection probability	dunif(-5,5)	runif(1,-1,1)
p0	Baseline detection probability	dunif(0,1)	runif(1,0,0.2)

Appendix 5. OPSCR model simulation test

We evaluated the reliability of our wolf OPSCR model under conditions resembling the Scandinavian wolf population (*i.e.* space use, population trajectory) and its monitoring (*e.g.* spatio-temporal intensity). We used the same habitat extent and detector configuration as in the empirical analysis. We simulated several multi-year datasets of individual detections with parameter values similar to those obtained in the OSPCR analysis of the Scandinavian wolf dataset (Tables A5.1 and A5.2). We created 20 data sets with the same set of parameter values. Even if identical parameter values were used in repeated simulations, variation in outcomes originating from random realizations of the demographic and observation processes led to different population development and therefore datasets. We then assessed performance (accuracy and precision) of the OPSCR model in retrieving the simulated values. Below is an outline of the steps involved in the simulation-based evaluation of the final OPSCR model:

1. Define the basic characteristics of the simulation. Here, we used the same spatial and temporal extent as the real data (Section 2.2.1). We also used the same detector characteristics, placement and covariates.
2. Simulate a population and the fates of its members according to demographic parameters, *i.e.* recruitment and cause-specific mortality (with associated dead-recovery).
3. Simulate the distribution of individual ACs in space each year, based on their location during the previous year and the effect of known pack density (as in the empirical data analysis).
4. Simulate individual detection histories; including a reduction in detectability with increasing distance from an individual location (see Appendix 3 and Section 2.3.3). Allow the baseline detection probability to vary according to individual and spatio-temporal covariates (*i.e.* individual state, previous detection, track length, country (Norway and Sweden) and distance to roads).
5. Fit the OPSCR model to the simulated data and retrieve estimates of parameters associated with population dynamics, spatial configuration, and the detection processes.
6. Repeat steps 2-5 for 20 independent simulations, each of which results in an alternative time series of population and observation data due to the stochasticity in the simulation process.
7. Compare the distribution of model-estimated parameter values over the 20 repetitions with the true value of each parameter used in the simulation.

Table A5.1. Summary of the demographic parameters used in the simulation study

Parameters	Demographic state			
	"alive other"	"alive scent-marking adult"	"dead legal"	"dead"
γ (Initial state probability)	0.20	0.8	0	0
r (Reproduction probability)	0	1.0	0	0
λ (Per capita recruitment rate)	0	1.1	0	0
Φ (Survival probability)	0.55	0.7	-	-
ψ (Transition probability)	0.40	-	-	-
h (Legal culling mortality)	0.10	0.1	-	-
w (Other mortality)	0.35	0.2	-	-

Table A5.2. Summary of the detection and other parameters used in the simulation study

Parameters	Year			
	2014	**2015**	**2016**	**2017**
$p0_1$ ("alive other")	0.03	0.06	0.07	0.08
$p0_2$ ("alive scent-marking adult")	0.04	0.065	0.07	0.09
β1 (idResponse)			0.4	
β2 (DistRoads)			-0.3	
β3 (Snow)			0.05	
β4 (Tracks)			0.3	
β5 (Country)			0.2	
σ (scale parameter)			10	
τ (dispSigma)			50	
β (PackDensity)			0.5	

To evaluate the ability of the OPSCR model to retrieve the simulated parameter values, we quantified the accuracy and precision of the different parameter estimates. As a measure of accuracy, we calculated the relative bias $(\Theta) = \frac{\hat{\theta}-\theta}{\theta}$, where $\hat{\theta}$ is the median of the posterior distribution of the parameter of interest and θ is the simulated value of the parameter, for all 20 repeated simulations associated with a given parameter set. As a measure of precision, we calculated the coefficient of variation $CV(\theta) = \frac{sd(\hat{\theta})}{\bar{\theta}}$ where $sd(\hat{\theta})$ and $\bar{\theta}$ are the standard deviation and mean of the posterior distribution of the parameter of interest, respectively.

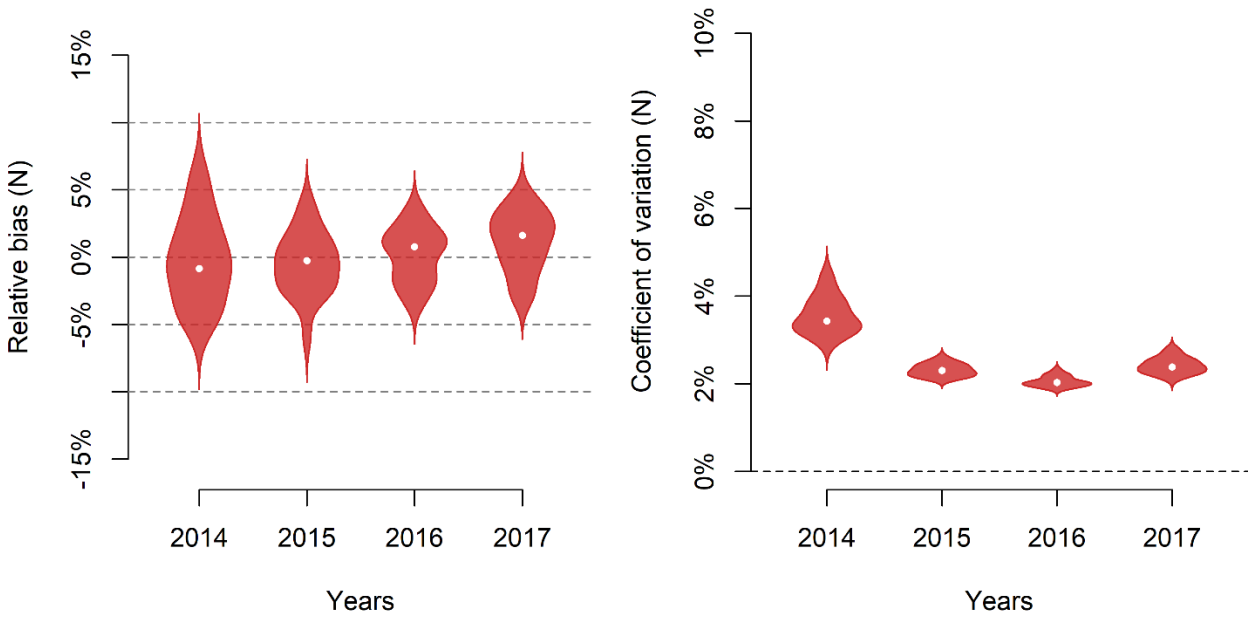

Figure A5.3. *Relative bias and coefficient of variation of OPSCR-derived estimates of population size based on 20 simulations.*

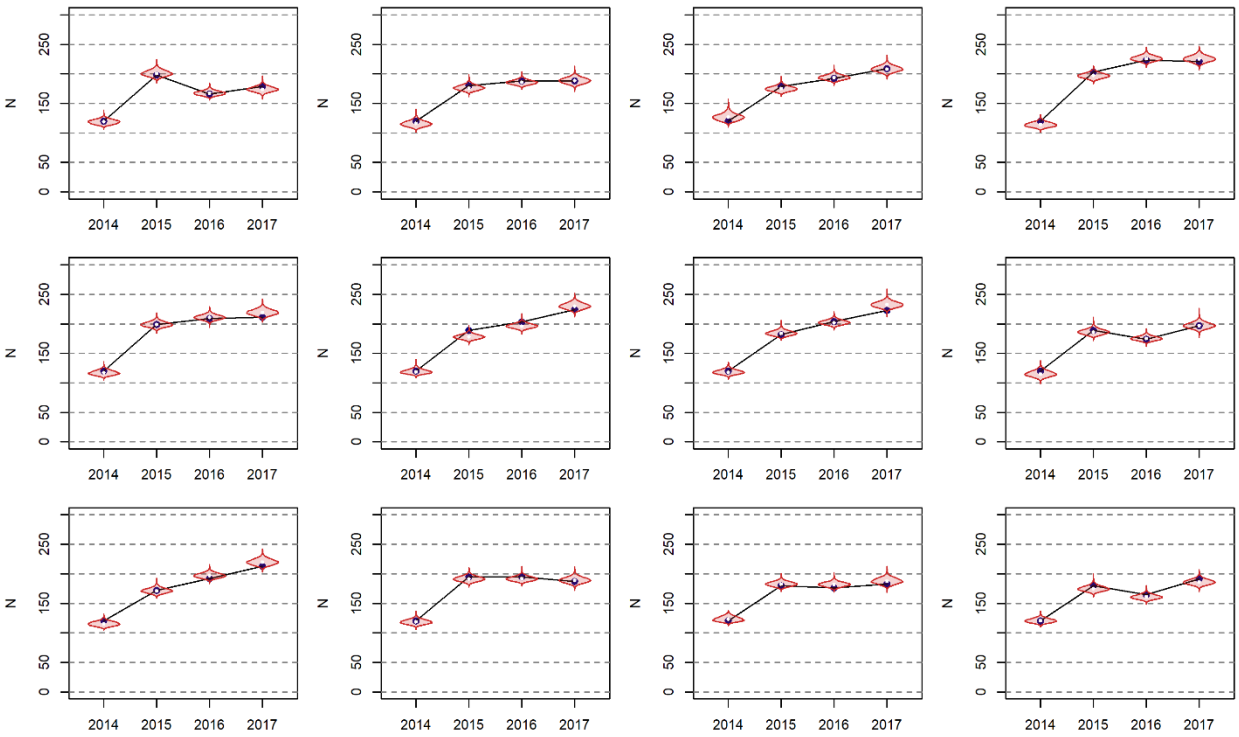

Figure A5.4. *Results for 12 example simulations. Violins show the OPSCR-estimated annual population sizes from simulated data; lines connect the "true" sizes of the simulated populations.*

Appendix 6. Bayesian posterior predictive checks

Bayesian Posterior predictive checks estimate the probability to obtain the dataset used in the analysis (*i.e.* the observed dataset) under the fitted model by comparing the value(s) of the observed dataset to the distribution of predicted datasets. A model able to *predict* new datasets resembling the original input data is considered to have a *good fit* or *good predictive power* (Gelman and Shalizi 2013). This comparison requires two steps:

1. Generate multiple predicted datasets from the fitted model to obtain a distribution of possible datasets following the fitted model.
2. Compare the observed dataset to the distribution of predicted datasets to assess the likelihood of the observed dataset being produced by the fitted model.

To generate *K* predicted datasets from the fitted model, we randomly picked *K* sets of parameter values from the posterior MCMC samples (*i.e. K* iterations). We then created a NIMBLE custom function (de Valpine et al. 2017) to use each of these *K* sets of parameter values to generate new datasets (y_{ijt}) from the OPSCR model. This last step was made possible by the NIMBLE built-in functionality "simulate" that draws random values for a specified set of nodes in the model from the set of values picked from the posterior samples (de Valpine et al. 2017).

We then visually compared the distribution of these predicted datasets to the observed dataset with respect to:

- the total number of detections per detector per year (Figure A6.1)
- the total number of detections per individual per year (Figure A6.2)

Comparisons revealed that, in the observed dataset, we obtained moderately (~3%) more detectors with zero detections than expected under the fitted model and less detectors with one or two (~32% and ~18.5% respectively) total number of detections. On the other hand, we observed no pronounced mismatch between the tails of the observed and predicted distributions. This pattern was similar for both males and females.

The discrepancy between the predicted and observed number of detections per individual was much lower for both males and females, with only a slight mismatch between the predicted and observed number of individuals with 0, 1 or 2 detections per year (~1.5%, ~1.6% and 14.5% respectively).

These results are encouraging, but further analyses are required to precisely quantify the goodness of fit of our model, and to assess potential consequences of poor fit for the accuracy and precision of our estimates.

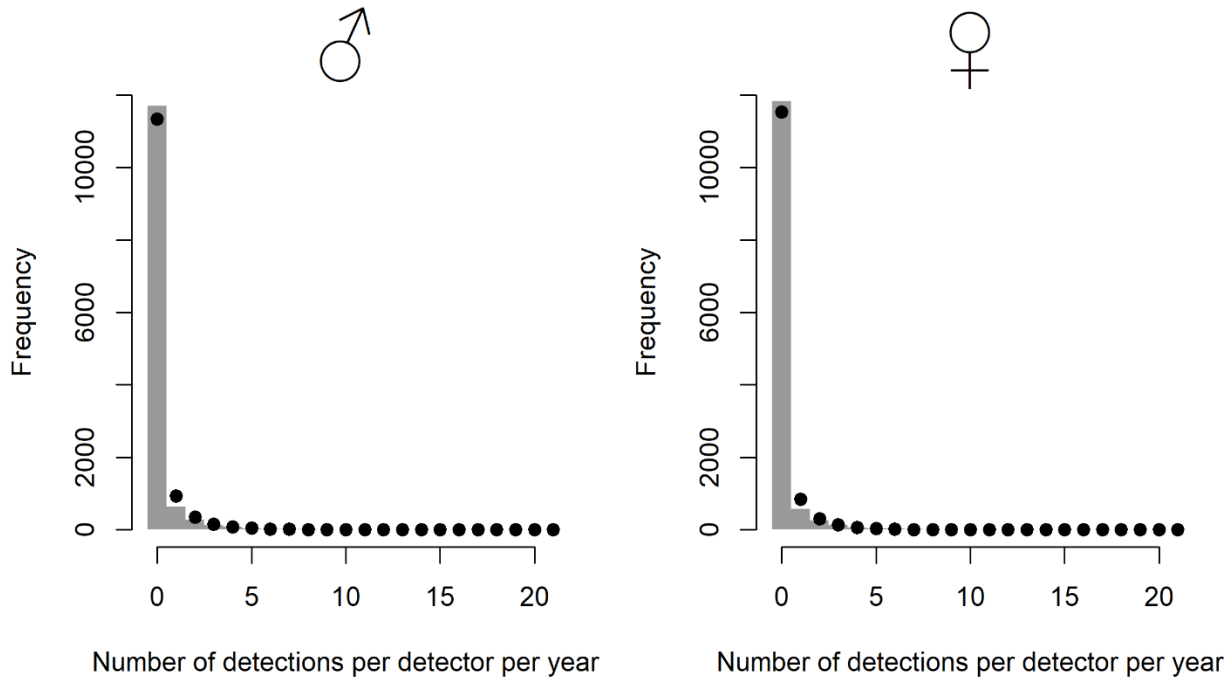

Figure A6.1. Distribution of the number of detections per detector per year in the original wolf dataset (grey bars) and in the predicted datasets from the fitted model; black points represent the median number of detections in the predicted data.

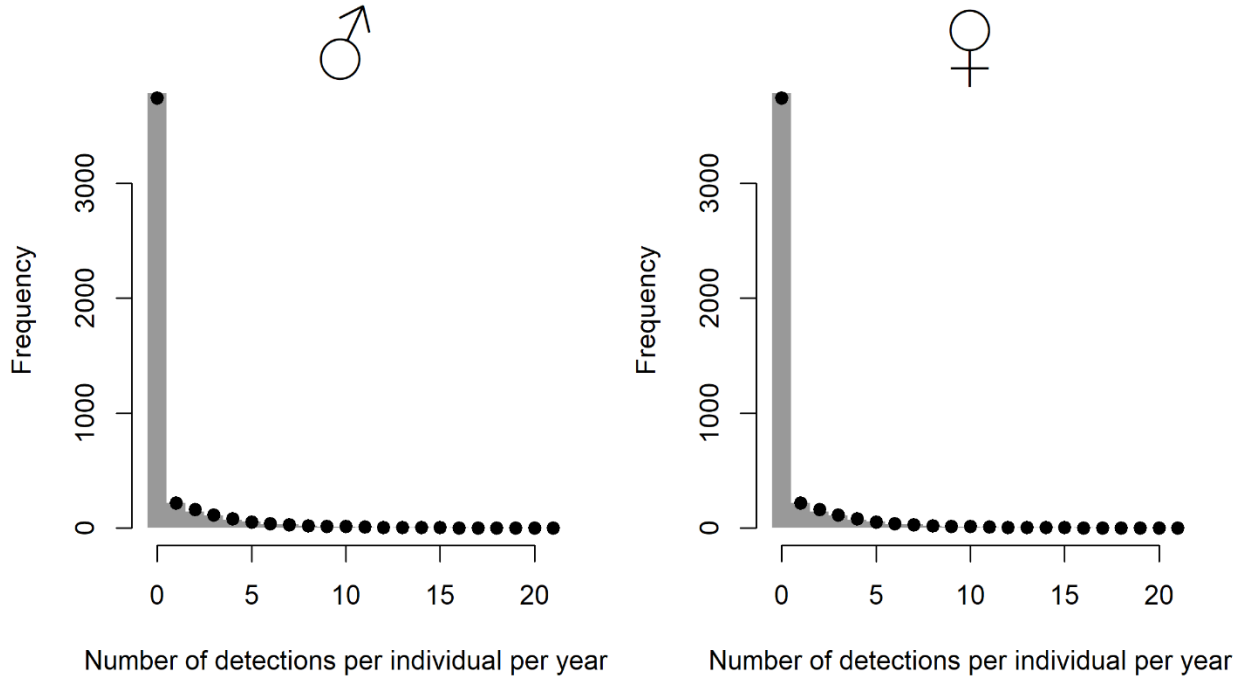

Figure A6.2. Distribution of the number of detections per individual per year in the original wolf dataset (grey bars) and in the predicted datasets from the fitted model; black points represent the median number of detections in the predicted data.

Appendix 7. Parameter estimates

Table A7.1 Population size estimates by country and year based on OPSCR-predicted activity center locations of wolves in Scandinavia

	2013	2014	2015	2016	2017
Sweden	308 (286 - 333)	350 (327 - 375)	298 (281 - 317)	323 (313 - 334)	310 (301 - 321)
Norway	60 (48 - 74)	71 (61 - 82)	70 (64 - 77)	79 (72 - 87)	91 (83 - 101)
TOTAL	368 (344 - 397)	421 (397 - 448)	368 (351 - 387)	402 (393 - 412)	401 (392 - 412)

Table A7.2 Population size estimates by sex and jurisdiction on Oct 1 2017 based on OPSCR-predicted activity center locations of wolves in Scandinavia. Not all counties are shown, therefore county estimates do not add up to national totals. Combined female-male estimates are obtained by joining the sex-specific posterior distribution. Shifts in the resulting median estimates explain occasional small deviations of the total from the sum of the sex-specific medians.

	Females	Males	Total
TOTAL	197 (191-205)	204 (198-212)	401 (392-412)
SWEDEN	149 (142-157)	161 (155-168)	310 (301-321)
Östergötland	1 (1-3)	2 (2-3)	3 (3-5)
Dalarna	26 (22-30)	29 (26-33)	55 (50-61)
Gävleborg	32 (30-34)	31 (28-33)	62 (59-66)
Jämtland	3 (1-7)	4 (2-8)	8 (4-13)
Orebro	16 (13-19)	14 (13-17)	30 (27-34)
Södermanland	2 (2-4)	10 (9-12)	12 (11-14)
Stockholm	3 (2-4)	2 (1-4)	5 (3-7)
Uppsala	3 (2-4)	1 (0-3)	4 (2-6)
Värmland	45 (40-50)	46 (41-51)	91 (84-98)
Västmanland	14 (12-16)	17 (14-21)	31 (27-35)
Västra Götaland	4 (2-7)	5 (3-8)	10 (6-14)
NORWAY	48 (42-55)	43 (37-50)	91 (83-101)
Østfold	4 (2-6)	5 (3-7)	9 (6-12)
Akershus	4 (3-6)	6 (5-7)	10 (8-12)
Hedmark	38 (33-43)	30 (25-36)	68 (61-76)
Sør-Trøndelag	1 (0-4)	1 (0-4)	2 (0-6)

Table A7.3 Estimates of the demographic parameters obtained from the wolf OPSCR model. Parameters represent transition rates from October 1 in one year to September 30 in the following year. Median estimates and 95% credible intervals (in parentheses) are shown for recruitment probability for individuals in state "unborn" (γ), survival (ϕ), transition from "Other" to "Scent-marking adult" (ψ), mortality due legal culling (h), and mortality due to other causes (w) are presented for males (M) and females (F) and for "Scent-marking adult" (State 3) and "other" (State 2) individuals. See Appendix 3 for a full description of the model parameters.

	State	2013-2014		2014-2015		2015-2016		2016-2017	
		M	F	M	F	M	F	M	F
γ	-	0.16 (0.12-0.20)	0.16 (0.12-0.20)	0.15 (0.11-0.19)	0.12 (0.08-0.16)	0.18 (0.14-0.22)	0.23 (0.18-0.27)	0.25 (0.21-0.30)	0.25 (0.20-0.31)
Φ	2	0.55 (0.44-0.65)	0.57 (0.45-0.69)	0.47 (0.38-0.56)	0.48 (0.37-0.58)	0.54 (0.44-0.63)	0.55 (0.44-0.67)	0.50 (0.42-0.59)	0.59 (0.50-0.67)
	3	0.66 (0.52-0.80)	0.64 (0.50-0.77)	0.64 (0.51-0.76)	0.68 (0.55-0.80)	0.69 (0.57-0.79)	0.64 (0.52-0.75)	0.55 (0.44-0.67)	0.59 (0.47-0.70)
Ψ	-	0.29 (0.19-0.41)	0.41 (0.27-0.55)	0.34 (0.23-0.46)	0.37 (0.24-0.51)	0.32 (0.22-0.44)	0.42 (0.29-0.57)	0.42 (0.30-0.54)	0.43 (0.32-0.55)
h	2	0.05 (0.03-0.10)	0.07 (0.04-0.13)	0.18 (0.12-0.24)	0.20 (0.13-0.28)	0.13 (0.08-0.20)	0.06 (0.03-0.13)	0.18 (0.12-0.25)	0.13 (0.08-0.20)
	3	0.08 (0.03-0.17)	0.09 (0.04-0.18)	0.10 (0.04-0.19)	0.10 (0.05-0.19)	0.08 (0.03-0.16)	0.09 (0.04-0.17)	0.10 (0.05-0.19)	0.10 (0.05-0.19)
w	2	0.40 (0.29-0.50)	0.35 (0.23-0.48)	0.35 (0.26-0.45)	0.32 (0.22-0.44)	0.33 (0.24-0.43)	0.38 (0.27-0.49)	0.31 (0.23-0.40)	0.28 (0.20-0.36)
	3	0.25 (0.13-0.40)	0.26 (0.13-0.40)	0.25 (0.15-0.38)	0.21 (0.11-0.34)	0.22 (0.14-0.34)	0.26 (0.16-0.38)	0.34 (0.23-0.45)	0.30 (0.20-0.41)

Table A7.4 Estimates of space use, movement, and covariate effect parameters obtained from the wolf OPSCR model. Shown are sex-specific parameters for the scale parameter of the detection function (σ), dispersal sigma (τ), effect of detected pack density on the spatial intensity of ACs location (β), effect of previous detection of individual on detection probability (β_1), effect of distance to the closest roads on detection probability (β_2), effect of average snow cover during the monitoring period on detection probability (β_3), and effect of search effort (track length) on detection probability (β_4). See Appendix 3 for a full description of the model parameters.

Parameter	**Sex**	
	Males	Females
$\boldsymbol{\sigma}$	7.96 (7.80-8.12)	7.62 (7.45-7.79)
$\boldsymbol{\tau}$	75.28 (70.94-80.96)	53.37 (49.62-56.74)
$\boldsymbol{\beta}$	0.47 (0.44-0.51)	0.51 (0.47-0.54)
$\boldsymbol{\beta_1}$	0.12 (0.02-0.23)	0.37 (0.26-0.48)
$\boldsymbol{\beta_2}$	-0.52 (-0.74-(-)0.33)	-0.85 (-1.11-(-)0.59)
$\boldsymbol{\beta_3}$	-0.01 (-0.10-0.08)	0.07 (-0.04-0.18)
$\boldsymbol{\beta_4}$	0.27 (0.24-0.31)	0.27 (0.23-0.30)

Table A7.5 Median estimates (with 95% credible interval) of the baseline detection probability obtained from the wolf OPSCR model. Estimates are presented for males (M) and females (F), "Others" and "Scent-marking adult", and each region (see Figure A7.1 for a visual representation of the regions). See Appendix 3 for full description of the model parameters.

		2013		2014		2015		2016		2017	
		M	F	M	F	M	F	M	F	M	F
NO1	Others	0.004 (0.001-0.009)	0.005 (0.002-0.013)	0.010 (0.003-0.022)	0.007 (0.002-0.017)	0.021 (0.013-0.034)	0.009 (0.005-0.017)	0.013 (0.007-0.025)	0.005 (0.002-0.012)	0.014 (0.010-0.019)	0.010 (0.007-0.015)
NO1	Scent-marking adult	0.012 (0.004-0.026)	0.004 (0.001-0.039)	0.009 (0.003-0.021)	0.019 (0.009-0.035)	0.012 (0.006-0.020)	0.013 (0.006-0.026)	0.008 (0.005-0.012)	0.009 (0.005-0.014)	0.020 (0.013-0.031)	0.015 (0.009-0.023)
SE1	Others	0.001 (0.001-0.002)	0.001 (0.001-0.002)	0.001 (0.001-0.002)	0.001 (0.001-0.002)	0.003 (0.002-0.004)	0.002 (0.001-0.003)	0.005 (0.004-0.006)	0.004 (0.003-0.005)	0.007 (0.006-0.008)	0.006 (0.005-0.007)
SE1	Scent-marking adult	0.004 (0.003-0.006)	0.002 (0.001-0.003)	0.004 (0.002-0.005)	0.002 (0.001-0.002)	0.005 (0.004-0.006)	0.003 (0.002-0.004)	0.012 (0.010-0.015)	0.008 (0.007-0.010)	0.016 (0.012-0.019)	0.007 (0.006-0.009)
SE2	Others	0.002 (0.001-0.003)	0.001 (0.000-0.003)	0.002 (0.001-0.003)	0.001 (0.000-0.002)	0.001 (0.000-0.002)	0.000 (0.000-0.001)	0.005 (0.003-0.008)	0.009 (0.007-0.013)	0.008 (0.005-0.011)	0.005 (0.003-0.008)
SE2	Scent-marking adult	0.003 (0.001-0.005)	0.003 (0.001-0.004)	0.002 (0.001-0.004)	0.002 (0.001-0.003)	0.005 (0.003-0.009)	0.001 (0.001-0.003)	0.019 (0.015-0.025)	0.010 (0.007-0.014)	0.020 (0.016-0.026)	0.012 (0.009-0.016)
NO2	Others	0.003 (0.002-0.005)	0.003 (0.001-0.006)	0.004 (0.003-0.006)	0.003 (0.002-0.005)	0.007 (0.005-0.009)	0.005 (0.004-0.008)	0.007 (0.005-0.010)	0.008 (0.006-0.010)	0.005 (0.004-0.007)	0.006 (0.004-0.008)
NO2	Scent-marking adult	0.007 (0.004-0.012)	0.004 (0.002-0.007)	0.006 (0.004-0.010)	0.005 (0.003-0.008)	0.007 (0.005-0.011)	0.008 (0.006-0.011)	0.012 (0.009-0.017)	0.009 (0.007-0.013)	0.017 (0.013-0.022)	0.009 (0.007-0.012)
SE3	Others	0.004 (0.002-0.009)	0.002 (0.001-0.006)	0.002 (0.001-0.004)	0.001 (0.000-0.003)	0.002 (0.001-0.005)	0.006 (0.003-0.012)	0.008 (0.005-0.011)	0.007 (0.005-0.010)	0.005 (0.004-0.007)	0.005 (0.004-0.007)

SE3	Scent-marking adult	0.006 (0.002-0.012)	0.010 (0.005-0.018)	0.004 (0.002-0.006)	0.004 (0.002-0.006)	0.008 (0.004-0.013)	0.003 (0.001-0.006)	0.017 (0.012-0.024)	0.014 (0.010-0.020)	0.021 (0.016-0.027)	0.017 (0.013-0.023)
SE4	Others	0.002 (0.001-0.003)	0.001 (0.001-0.002)	0.001 (0.001-0.001)	0.001 (0.001-0.002)	0.002 (0.001-0.003)	0.002 (0.001-0.003)	0.002 (0.002-0.003)	0.003 (0.002-0.004)	0.005 (0.004-0.006)	0.005 (0.004-0.007)
SE4	Scent-marking adult	0.002 (0.002-0.004)	0.002 (0.001-0.002)	0.003 (0.002-0.005)	0.002 (0.001-0.003)	0.005 (0.004-0.007)	0.003 (0.002-0.004)	0.010 (0.008-0.013)	0.007 (0.005-0.009)	0.014 (0.012-0.017)	0.006 (0.005-0.008)

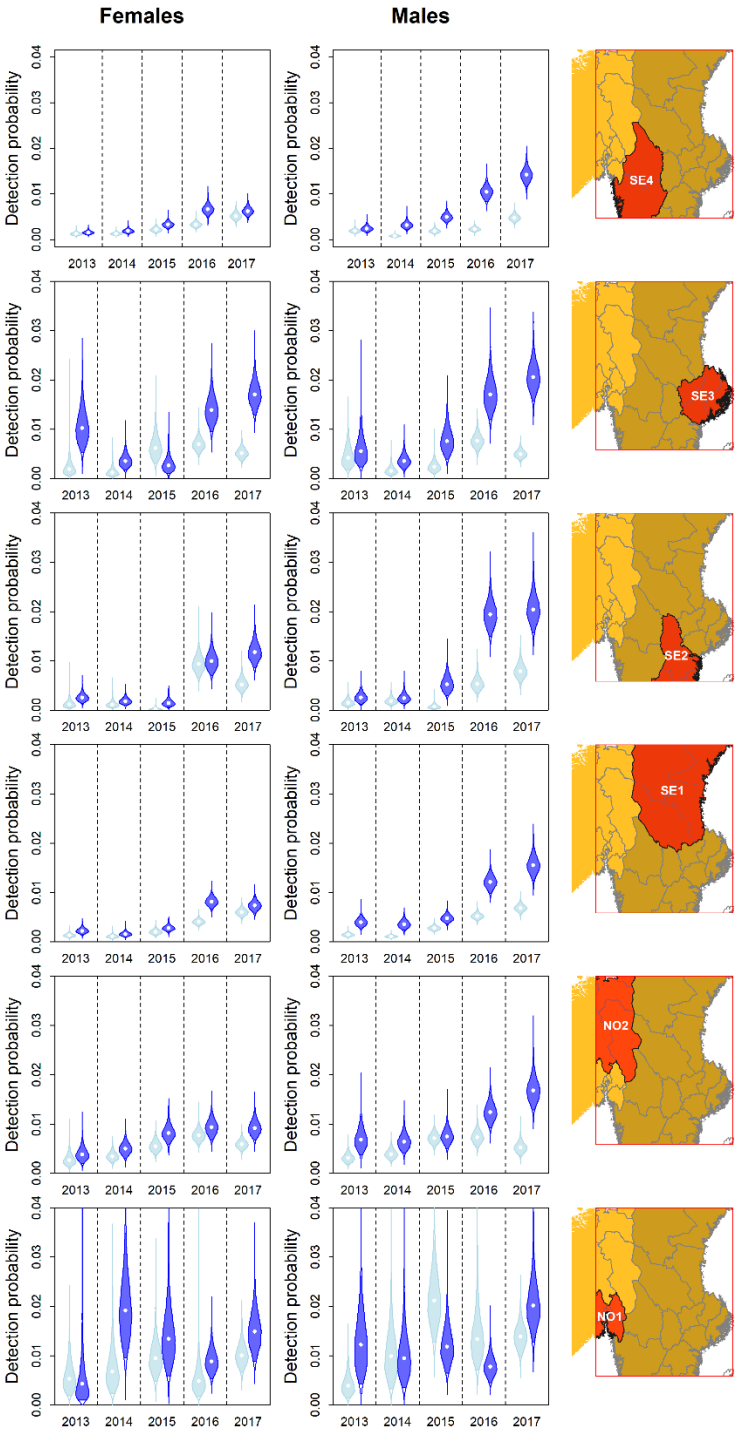

Figure A7.6. *Baseline detection probability (p_0) estimated by the OPSCR model. Violins show the distribution of the posterior samples, white dots indicate the median, and areas with solid shading represent the 95% credible interval. Violin colors indicate detection probability estimates associated with scent-marking adults (dark blue) and other individuals (light blue). Results are separated into panels based on sex and regions (counties or groups of counties, as shown in the maps in the right column). Estimates are shown for the mean values of detection covariates (snow cover, distance from road, and search track length).*

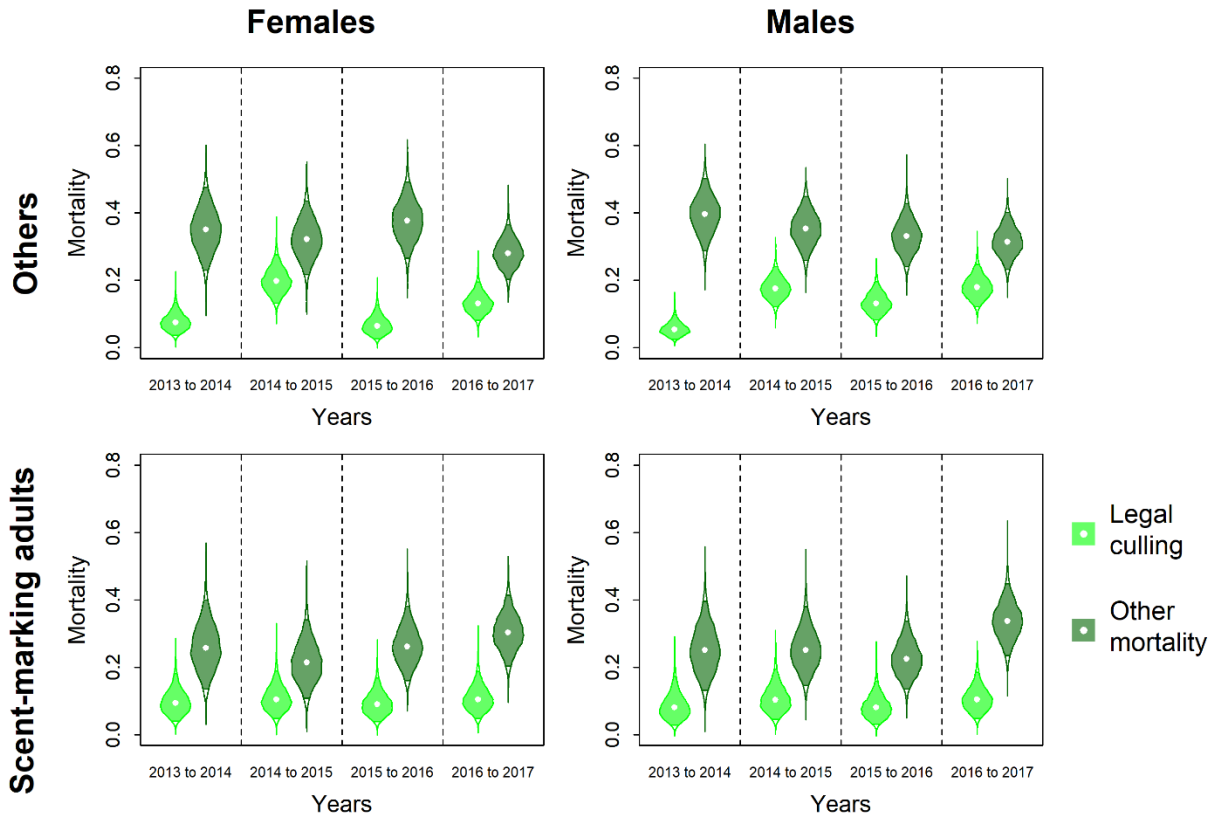

Figure A7.7. *Cause-specific mortality estimated by the OPSCR model. Violins show the distribution of posterior samples, white dots indicate the median, and regions with solid shading represent the 95% credible interval. Estimates are for legal culling and all other causes of mortality (including deaths that were not detected), separated into panels based on sex and individual states. Annual mortality refers to all deaths occurring between October 1 in one year and September 30 the following year.*

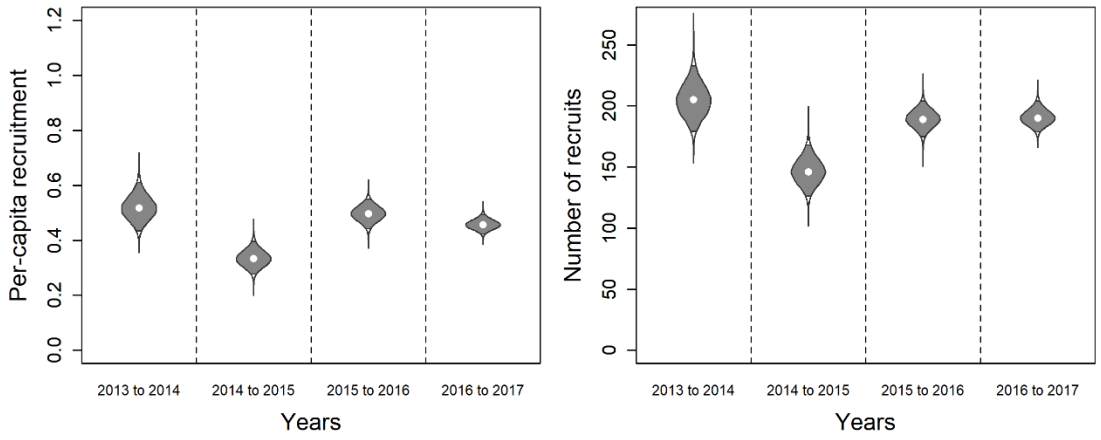

Figure A7.8. *Annual per-capita recruitment (based on individuals present in the population during the previous year) and number of recruits estimated by the OPSCR model. Violins show the distribution of the posterior samples, white dots indicate the median, and regions with solid shading represent the 95% credible interval. Recruitment, as estimated by the OPSCR model is the combined probability of an individual being born and surviving until the start of the monitoring season (October 1) in its birth year.*

References with the appendices

Bischof, R., J. E. Swenson, N. G. Yoccoz, A. Mysterud, and O. Gimenez. 2009. The magnitude and selectivity of natural and multiple anthropogenic mortality causes in hunted brown bears. Journal of Animal Ecology 78:656–665.

Chapron, G., C. Wikenros, O. Liberg, L. Svensson, M. Åkesson, J. Månsson, B. Zimmermann, C. Milleret, P. Wabakke, and H. Sand. 2015. Population estimates for the Scandinavian wolf population and sample-based monitoring – development of a new method. Rapport från Viltskadecenter, SLU 2015-5.

Chapron, G., C. Wikenros, O. Liberg, P. Wabakken, Ø. Flagstad, C. Milleret, J. Månsson, L. Svensson, B. Zimmermann, M. Åkesson, and H. Sand. 2016. Estimating wolf (Canis lupus) population size from number of packs and an individual based model. Ecological Modelling 339:33–44.

Ergon, T., and B. Gardner. 2014. Separating mortality and emigration: modelling space use, dispersal and survival with robust-design spatial capture–recapture data. Methods in Ecology and Evolution 5:1327–1336.

Gardner, B., R. Sollmann, N. S. Kumar, D. Jathanna, and K. U. Karanth. 2018. State space and movement specification in open population spatial capture-recapture models. Ecology and Evolution 0.

Gelman, A., and C. R. Shalizi. 2013. Philosophy and the practice of Bayesian statistics. British Journal of Mathematical and Statistical Psychology 66:8–38.

Gimenez, O., V. Rossi, R. Choquet, C. Dehais, B. Doris, H. Varella, J.-P. Vila, and R. Pradel. 2007. State-space modelling of data on marked individuals. Ecological Modelling 206:431–438.

Illian, J., A. Penttinen, H. Stoyan, and D. Stoyan. 2008. Statistical Analysis and Modelling of Spatial Point Patterns. Wiley.

Kery, M., and M. Schaub. 2011. Bayesian Population Analysis using WinBUGS: A Hierarchical Perspective. Elsevier Science.

Mattisson, J., H. Sand, P. Wabakken, V. Gervasi, O. Liberg, J. C. Linnell, G. Rauset, and H. Pedersen. 2013. Home range size variation in a recovering wolf population: evaluating the effect of environmental, demographic, and social factors. Oecologia 173:1–13.

Milleret, C., P. Dupont, C. Bonenfant, H. Brøseth, Ø. Flagstad, C. Sutherland, and R. Bischof. 2018a. A local evaluation of the individual state-space to scale up Bayesian spatial capture-recapture. Ecology and evolution 9:352–363.

Milleret, C., P. Dupont, H. Brøseth, J. Kindberg, J. A. Royle, and R. Bischof. 2018b. Using partial aggregation in spatial capture recapture. Methods in Ecology and Evolution 9:1896–1907.

Royle, J. A., R. M. Dorazio, and Link W.A. 2007. Analysis of multinomial models with unknown index using data augmentation. Journal of Computational and Graphical Statistics 16(1):67–85.

Royle, J. A., K. U. Karanth, A. M. Gopalaswamy, and N. S. Kumar. 2009. Bayesian inference in camera trapping studies for a class of spatial capture–recapture models. Ecology 90:3233–3244.

Schwarz, C. J., and A. N. Arnason. 1996. A General Methodology for the Analysis of Capture-Recapture Experiments in Open Populations. Biometrics 52:860–873.

Seber, G. A. F. 1965. A Note on the Multiple-Recapture Census. Biometrika 52:249–259.

Svensson, L., P. Wabakken, I. Kojola, E. Maartmann, T. Strømseth, M. Åkesson, and Ø. Flagstad. 2014. Varg i Skandinavien och Finland: Slutrapport fraøninventering av varg vintern 2013–2014. Høgskolan i Hedmark.

Svensson, L., P. Wabakken, E. Maartmann, M. Åkesson, and Ø. Flagstad. 2015. Inventering av varg vintern 2014-2015. Inventeringsresultat för stora rovdjur i Skandinavien 1-2015.

Svensson, L., P. Wabakken, E. Maartmann, M. Åkesson, and Ø. Flagstad. 2017. Inventering av varg vintern 2016-2017 / Bestandsovervåking av ulv vinteren 2016-2017. Page Bestandsstatus for store rovdyr i Skandinavia.

Svensson, L., P. Wabakken, E. Maartmann, M. Åkesson, and Ø. Flagstad. 2018. Bestandsovervåking av ulv vinteren 2017-2018 / Inventering av varg vintern 2017-2018. Page Bestandsstatus for store rovdyr i Skandinavia.

de Valpine, P., D. Turek, C. J. Paciorek, C. Anderson-Bergman, D. T. Lang, and R. Bodik. 2017. Programming With Models: Writing Statistical Algorithms for General Model Structures With NIMBLE. Journal of Computational and Graphical Statistics 26:403–413.

Wabakken, P., Å. Aronson, H. Sand, H. Rønning, and I. Kojola. 2004. Ulv i Skandinavia. Statusrapport for vinteren 2002-2003. Høgskolen i Hedmark, Viltskadecenter, Grimsö forskningsstation, Vilt- og fiskeriforskningen, Oulu. Høgskolen i Hedmark Oppdragsrapport 2.

Wabakken, P., Å. Aronson, H. Sand, Steinset, O.K., and I. Kojola. 2001. Ulv i Skandinavia. Statusrapport for vinteren 2000-2001. Høgskolen i Hedmark, Viltskadecenter, Grimsö forskningsstation, Vilt- og fiskeriforskningen, Oulu. Høgskolen i Hedmark. Oppdragsrapport 1.

Wabakken, P., Å. Aronson, H. Sand, Steinset, O.K., and I. Kojola. 2002. Ulv i Skandinavia. Statusrapport for vinteren 2001-2002. Høgskolen i Hedmark, Viltskadecenter, Grimsö forskningsstation, Vilt- og fiskeriforskningen, Oulu. Høgskolen i Hedmark Oppdragsrapport 2.

Wabakken, P., L. Svensson, E. Maartmann, M. Åkesson, and Ø. Flagstad. 2016. Bestandsovervåking av ulv vinteren 2015-2016. Page Bestandsstatus for store rovdyr i Skandinavia.